Gradual segregation of Adult Stem Cells and Niche cells during development from common precursors under the guidance of graded extracellular signals

Amy Reilein[#*], Helen V. Kogan[#], Rachel Misner, Karen Sophia Park, Daniel Kalderon*

Department of Biological Sciences, Columbia University, New York, USA

[#] equal first authors

* corresponding authors: areilein@gmail.com, ddk1@columbia.edu

Summary

Adult stem cell function relies on the prior specification and organization of appropriate numbers of stem cells and supportive niche cells during development. Insights into those developmental processes could facilitate the synthesis of organoid mimics. Drosophila Follicle Stem Cells (FSCs) present an amenable paradigm with many similarities to mammalian gut stem cells. In an adult germarium a central domain of about 16 FSCs produces a posterior stream of transit-amplifying Follicle Cells (FCs), which encapsulate mature germline cysts to support egg development and, from their anterior face, quiescent Escort Cells (EC), which support the maturation of germline cysts. The behavior of FSCs is guided in part by niche signals produced by ECs and by a specialized polar cell FC derivative. Thus, ECs and FCs are both adult stem cell products and niche cells. Here we show by lineage analyses that adult ECs, FSCs and FCs derive from common precursors during pupal development. We infer that disparities in initial anterior-posterior (AP) precursor location followed by limited dispersal of progeny leads to a gradual acquisition of distinct fates determined by final AP location, with progeny of a single precursor commonly straddling EC and FSC, FSC and FC, or all three territories through most of pupal development. Direct visualization of pupal ovaries, including live imaging revealed a transient population of FC precursors posterior to the developing germarium awaiting emergence of the most mature germline cyst. The consequent budding process was quite different from the budding of egg chambers in adults. An anterior to posterior gradient of Wnt signaling develops shortly after pupariation. Loss of pathway activity cell autonomously resulted in more posterior adult progeny fates, while increased pathway activity elicited the opposite response, suggesting that stronger Wnt signaling favors anterior migration. Clearly detectable JAK-STAT pathway activity emerges only halfway through pupation after polar cells form, and spreads from posterior to anterior. Loss of JAK-STAT activity had similar consequences to increased Wnt pathway activity, drastically reducing FSC and FC production cell autonomously, while increased JAK-STAT activity promoted excessive precursor proliferation. We conclude that FSCs develop in co-ordination with their niche and product cells, that specification of stem cell identity is gradual, subject to stochastic influences and guided by graded extracellular signals, presaging similar regulation of adult stem cell behavior by the same pathways.

Introduction

Adult stem cells must be established in suitable numbers and niche environments during development to ensure that their activity is properly regulated and suffices to maintain the relevant adult tissue. Identifying stem and niche cell precursors and ascertaining how their coordinated development is organized would provide an essential foundation for understanding how the normal process may go awry, potentially conferring a subsequent deficiency in tissue repair or cancer susceptibility. In addition, it would facilitate the creation ex vivo of functional stem cell units as organoids from pluripotent stem cells, which can typically only be guided in isolation towards immature (non-adult) cell fates.

The development of most terminally differentiated adult cell types generally results from a series of successive definitive and irreversible decisions that are stabilized by potentially long-lasting shifts in gene expression and chromatin modification [citations]. The development of adult stem cells has not been studied extensively and may differ significantly from that paradigm because stem cells typically continue to proliferate in adulthood and often exhibit malleable relationships with their products, with the potential for marked changes in interconversion rates in either direction.

Drosophila ovarian Follicle Stem Cells (FSCs) present a particularly interesting paradigm because the organization, behavior and regulation of these adult stem cells has been studied quite thoroughly to reveal many similarities to mammalian gut stem cells as well as a variety of interesting, potentially prototypical features (Gehart and Clevers, 2019; Hayashi et al., 2020; Reilein et al., 2017). Notably, FSCs are maintained by a form of population asymmetry wherein division and differentiation are not generally coupled (Reilein et al., 2018b), FSCs directly produce two instantaneously distinct types of cells, both of which produce important niche signals, and the proliferation rates and immediate differentiation potential of FSCs is heterogeneous but spatially organized. All of these behaviors are largely regulated by extracellular signals that are graded along the major (anterior-posterior) physiological axis (Reilein et al., 2017; Vied and Kalderon, 2009). FSCs are also of special interest because they must coordinate with germline cells, fueled by nearby Germline Stem Cells (GSCs) to produce functional products during oogenesis (Hayashi et al., 2020; Kahney et al., 2019; Waghmare and Page-McCaw, 2018). The mechanisms of coordination in the adult are currently not well understood but must rely on an organization that is established during development (Gilboa, 2015).

In the adult ovary, GSCs and FSCs are housed in the most anterior region of each of the 30-40 ovarioles, known as the germarium (Fig. 1J) (Hayashi et al., 2020). Somatic Terminal Filament (TF) and Cap Cells at the anterior of the germarium are stable sources of niche signals for GSCs and FSCs, with GSCs directly contacting Cap Cells. GSC Cystoblast daughters divide four times with incomplete

cytokinesis to yield a progression of 2-, 4-, 8- and 16-cell germline cysts. Their maturation is accompanied by posterior movement and depends on interactions with neighboring quiescent, somatic Escort Cells (ECs) (Kirilly et al., 2011). The most anterior and posterior ECs also act as niche cells for GSCs and FSCs, respectively (Hayashi et al., 2020; Sahai-Hernandez and Nystul, 2013; Waghmare and Page-McCaw, 2018; Wang and Page-McCaw, 2018). A rounded stage 2a sixteen cell cyst loses EC contacts as it forms a lens-shaped stage 2b cyst spanning the width of the germarium and subsequently recruits FCs, which characteristically express high levels of the surface adhesion protein, Fasciclin 3 (Fas3), from the most posterior layer of FSCs. The stage 2b cyst then rounds to a stage 3 cyst as surrounding FCs proliferate to form an epithelium and segregate specialized polar and stalk cells, which allow budding of the FC-enveloped cyst as an egg chamber from the posterior of the germarium (Duhart et al., 2017). Budding occurs roughly every 12h in well-fed flies. Egg chambers progressively enlarge and mature towards egg formation and deposition as they move posteriorly.

There are about 14-16 FSCs, which reside in three rings or layers around the inner germarial surface, between ECs and FCs on the AP axis (Fig. 1J) (Hayashi et al., 2020; Reilein et al., 2017). The most posterior FSCs directly become FCs, while anterior FSCs directly become ECs but FSCs also exchange AP locations, allowing a single FSC lineage to include both ECs and FCs. Individual FSCs are frequently lost and frequently amplify with no evident temporal or functional link between division and differentiation, so that the representation and output (of ECs and FCs) of any one FSC lineage is highly variable and stochastic.

Previous studies have outlined how germline and somatic ovary precursors are first selected during embryogenesis, then migrate and coalesce to form a nascent gonad (Jemc, 2011; Murray et al., 2010). The subsequent morphological organization of ovaries, constituent cell types and some information about relevant signals has been described up to the end of larval development (Gilboa, 2015; Godt and Laski, 1995). Understanding of pupal development is based on a series of electron micrographs and a description of some key morphological processes (Cohen et al., 2002; Godt and Laski, 1995; Irizarry and Stathopoulos, 2015; King et al., 1968; Valer et al., 2018) but had been limited, until recently, by technical difficulties associated with dissecting and imaging pupal ovaries (Park et al., 2018). Here we use morphological examination of developing pupal ovaries through fixed and live images, as well as cell lineage studies over this period to examine how adult FSCs, ECs and FCs are produced and organized from precursors present at the end of larval stages.

We find that there are some dedicated EC precursors at the start of pupation but most of the remaining precursors give rise to all three types of cell (ECs, FSCs and FCs). Over time, EC production declines as their precursors adopt the quiescent state of adult ECs, and the population of FC-only precursors increases. Meanwhile, a significant number of FSC precursors that no longer also produce

adult ECs emerge during the second half of pupation but those precursors still also produce FCs in newly-eclosed adults. At no stage is there a significant population of precursors that produce only FSCs. Instead, the key organizing principle guiding fate outcomes appears to be the distribution of precursors along the AP axis with limited, likely stochastic, subsequent changes in location of their progeny; only the final AP locations of cells at eclosion determine their identity.

During the first half of pupation, a subset of FC precursors, which we named Extra-Germarial Crown (EGC) cells, accumulates posterior to the interspersed germline and somatic cells of the germarium before engaging in a remarkable choreography, captured by live imaging, to form and populate the first egg chamber. After budding the first two egg chambers, the germarium adopts an adult appearance, suggesting that the adult organization is nearly complete.

By genetic manipulation of marked precursor lineages, stronger Wnt signaling, which is normally graded from anterior to posterior through most of pupal development, was found to favor anterior cell fates, presumably reflecting net anterior migration of precursors. Conversely, JAK-STAT signaling, which forms a gradient from posterior to anterior during the second half of pupation, was found to be important for acquisition of posterior FSC and FC fates, and also could greatly alter precursor proliferation rates.

Thus, the segregation of stem cells from niche cells in this paradigm is a gradual process, involving continued input from graded signaling sources and apparently stochastic fluctuations that affect AP location, rather than a rigidly imposed demarcation of different cell types delivered at a fixed time. The derivation of appropriate numbers of ECs and FSCs is assured in part by their emergence from shared precursors and from an evolving AP gradient of proliferation. These same characteristics ensure the normal AP organization of these cell types as a small initial population of precursors expands posteriorly from its anterior origins.

Results

Outline of ovary development

We dissected and imaged developing ovaries during pupation, highlighting germline cells with Vasa antibody, Terminal Filament and Cap cells with antibody to Lamin-C, and somatic ICs (and Cap Cells) with antibody to Traffic Jam (TJ) in order to provide a systematic descriptive timeline (Fig. 1). The germaria within each ovary develop at slightly different rates (from medial to lateral) and the overall duration of pupation can vary significantly, leading to some differences in the reported timing of critical stages (Cohen et al., 2002; Lai et al., 2017; Li et al., 2019). In common with other studies, we assign "0h APF" as the time when larvae cease moving (pupariation) and used that event to collect animals at known intervals after pupariation. Animals mostly eclosed five days later (120h APF). The first egg chamber had budded from about half of all germaria at about 56h APF (Fig. 1H).

Ovary organization has a clear temporal progression from anterior (generally termed apical at early stages) to posterior ("basal") (Fig. 1) (Gilboa, 2015; Godt and Laski, 1995). By the end of the third larval instar, each ovary has 15-20 anterior stacks of non-dividing Terminal Filament (TF) cells (Fig. 1J), which characteristically express Lamin-C but not Traffic Jam (TJ) (cyan arrowheads in Fig. 1D-F) (Godt and Laski, 1995; Panchal et al., 2017; Sahut-Barnola et al., 1996). "Apical cells" (white arrowheads, Fig. 1A, G), initially anterior to the TF stacks migrate towards the posterior (basally), first separating each TF stack and then entire developing ovarioles over the next 48h as they form an epithelial sheath lined by a basement membrane (Cohen et al., 2002). The most posterior "basal cells" express Fasciclin 3 (Fas3), initially in a patchy pattern (pink arrowheads, Fig. 1B, C) (Lai et al., 2017). Some of these cells later adopt an epithelial appearance, followed by progressive cell intercalation from posterior to anterior, to form a basal stalk (pink arrowheads, Fig. 1E-G) at the posterior end of each developing ovariole (Fig. 1J) (Godt and Laski, 1995; Vlachos et al., 2015).

Between the TFs and basal cells are developing germaria containing germline cells (green in Fig. 1) and somatic cells (white in Fig.1A-I). Six of these somatic cells surround the most posterior TF cell, the Transition Cell (Panchal et al., 2017), and become non-dividing Cap Cells (Fig. 1J), expressing Lamin-C and TJ shortly after the larval/pupal transition in response to Notch signaling and an ecdysone pulse (Gancz and Gilboa, 2013; Gancz et al., 2011; Panchal et al., 2017; Song et al., 2007; Yatsenko and Shcherbata, 2018). Primordial germline cells (PGCs) that contact Cap Cells largely remain in position to become adult Germline Stem Cells (GSCs) (Asaoka and Lin, 2004; Zhu and Xie, 2003). The remaining PGCs will develop similarly to adult Cystoblasts to produce 2-, 4-, 8- and finally 16-cell germarial cysts during pupation. The somatic cells posterior to Cap Cells in the developing germarium

are interspersed amongst germline cells and were therefore named Intermingled Cells (ICs) (Fig. 1J). These cells express TJ (white in Fig. 1A-I) but not Lamin C or Fas3 (both red in Fig. 1B-I) at pupariation, allowing a clear distinction from Cap Cells and basal stalk cells, respectively (Gilboa, 2015; Lai et al., 2017; Panchal et al., 2017). It has generally been assumed that ICs are the source of adult ECs (Gilboa, 2015) but neither this relationship nor the source of FSCs and FCs in newly-eclosed adults has been defined experimentally. Here, we use lineage analyses and the changing morphology of developing ovarioles during pupation to investigate the origin of adult somatic stem and niche cells.

Spatially organized progression of germline differentiation

The progress of germline development was monitored by by using Hts antibody (red in Fig. 2) to reveal a rounded spectrosome in single cells or the branched shape of the fusome, which connects Vasa-marked germline cells in a cyst (green in Fig. 2), and by incubating samples with EdU to assess DNA replication as a proxy for cell division (Fig. S1). Primordial Germ Cells (PGCs) do not initiate differentiation before late larval stages due to the repressive action of ligand-free ecdysone receptor and Broad transcription factor targets in somatic cells (Gancz et al., 2011). Thereafter, anterior PGCs receive Dpp signals from newly-formed Cap cells that prevent differentiation, allowing them to become adult GSCs, while posterior PGCs start to express the early differentiation marker, Bam-GFP in wandering third instar larvae just prior to pupariation, co-incident with a strong ecdysone pulse (Gancz et al., 2011; Zhu and Xie, 2003). A short time later, some branched fusomes are seen in posterior PGCs, indicating incomplete divisions with incomplete cytokinesis to form cysts with 2 or more cells (Gancz et al., 2011; Li et al., 2019). The progression of germline differentiation initiated in posterior PGCs during pupation has not been described.

We observed 2-cell cysts at 0h APF, cysts of up to 8 cells by 12h APF and sixteen cell cysts at 18h APF (Fig. 2A-C). Progressively larger cysts were arranged, with few exceptions, from anterior to posterior from 18h APF onwards; this was particularly clear in samples from 24h to 48h APF (Fig. 2D-F). Individual germaria within a developing ovary exhibited different degrees of progression, together with AP elongation of the germarium to accommodate increasingly large germ cell units, and in some cases germline cells had migrated posteriorly out of the germarial region (Fig. 2A-D). Multiple sixteen cell cysts were seen in individual germaria by 36h APF. The most posterior location included two cysts side by side in germaria at 24h APF but only a single cyst occupied that position in most cases by 36h APF and in all germaria by 48h APF (Fig. 2D-F). Consistent with these observations of cyst progression and location, EdU labeling was often seen in the most posterior cyst(s) up to 24h but rarely at 36h, while at 48h even the second most posterior cyst in the germarium rarely incorporated EdU

(Fig. S1A-D). Our observations reveal a progression of germline differentiation that is spatially organized along the AP axis during the first 48h APF, at which time the organization of germline cysts resembles that in the adult up to a stage 2b cyst (Fig. 1J).

Follicle Stem Cells and Escort Cells derive from a shared precursor

We used lineage analysis to learn about the specification of ECs, FSCs and FCs from precursors during pupal development. We chose MARCM clonal analysis (Lee and Luo, 2001) because positive cell marking greatly facilitates scoring all cells in a clone. We used a mild heat-shock to induce clones at defined times via a heat-shock inducible Flp recombinase transgene (*hs-flp*) to target all dividing precursors without bias and to try to produce clones derived from a single marked cell per ovariole. Maturation of a strong GFP MARCM signal in adult and developing ovarioles requires almost 4d. We therefore dissected ovarioles from adults 2d after eclosion ("+2d"), having induced clones daily (in separate experiments) between 6d and 2d before eclosion ("-6d" to "-2d"). Each ovariole was scored for the number of FSCs (defined as within the three layers of somatic cells anterior to the border of Fas3 staining) (Fig. 1J), the number of ECs (classified as region 1 or 2a, according to AP location) and for the presence of marked FCs in the germarium and first two egg chambers, by imaging and archiving complete confocal z-stacks (Fig. 3). Marked TF and Cap Cells were also noted. Clones were classified according to inferred cell types present at the time of eclosion (see Methods for extrapolating data from +2d adults to 0d adults).

The average number of labeled ECs and FSCs in a marked adult germarium decreased when clones were induced at progressively later stages (from an average of 8.1 at -6d to 2.0 at -2d) and very few marked clones were observed in the absence of heat-shock, consistent with almost all clones arising at the time of deliberately administered heat-shock and continued division of precursors through pupal development. As expected, TF cells were almost never labeled and CC labeling was seen only at the earliest times of induction (3% of clones at -5d) because these cells have already differentiated shortly before (TFs) or just after (CCs) the larval/pupal transition and the MARCM method only labels dividing cells.

Strikingly, almost all early-induced clones (from -6d to -4d) that included marked FSCs also contained marked ECs ("EC/FSC clones") (Fig. 3A, D-G) (Table 1). Clones containing only marked ECs ("EC only") were seen at each time of clone induction, while a high frequency of clones with marked FSCs but no marked ECs ("FSC only") was evident only when induced at -3d or -2d (Fig. 3A, K). These observations immediately suggested that most adult FSCs derive from a dividing precursor that gives

rise to both ECs and FSCs. During the second half of pupation an increasing proportion of the products of early EC/FSC precursors produce FSCs but no ECs.

Relative location of precursors along AP axis instructs fate

We found that marked cells in an adult germarium were generally clustered in the AP dimension, presumably centered on AP locations determined by the position of the first marked progenitor cell. This can be seen for all times of clone induction tested, from individual images (Fig. 3D-K) and also numerically after classifying locations more finely by counting marked region 1 (r1; most anterior) and region 2a (r2a) ECs separately. Of all clones (induced from -6d to -2d) containing more than one cell and at least one r1 EC, 35% contained no other cell type, 19% included also only r2a ECs, while only 8% also included only FSCs. Thus, sisters of a region 1 EC are most commonly only in region 1; they are also more commonly found in region 2a than in the more posterior FSC region, even though the total frequency of clones with region 2a ECs (54%) and FSCs (57%) were similar (Fig. 3B). Conversely, of all clones (induced from -6d to -2d) containing at least one FSC, 25% contained no ECs, 18% included also only r2a ECs, while only 11% also included only r1 ECs, even though the total frequency of clones with r1 ECs (68%) was higher than for r2a ECs (54%) (Fig. 3C). These observations support the hypothesis that precursors occupy significantly different AP positions throughout pupal development, their progeny undergo stochastic movement in either direction but still remain relatively close in the AP dimension and cell identity (r1 EC, r2a EC or FSC) is set by their AP location at eclosion. By adulthood this identity includes starkly different behaviors of quiescence (ECs) or proliferation (FSCs).

EC precursor division declines from the anterior at mid-pupation

For each time of clone induction, we summed the total number of marked FSCs and ECs (split into r1 and r2a) over all clones (Table 2). The ratio of marked ECs (r1 or r2a) to FSCs reports the relative number of the different cell types subsequently produced from dividing precursors. The absolute number of ECs to be made from dividing precursors in a single germarium was then calculated by assuming that each adult germarium has sixteen FSCs and that FSC precursors, like FSCs themselves, do not cease dividing (hence, prior to eclosion there are always 16 adult FSCs to be made from dividing precursors) (Table 2). Importantly, this calculation is based on scoring all labeled

cells over all clones and is therefore equally valid whether the scored cells in an ovariole derive from a single marked cell or from more than one marked cell.

The number of ECs in an adult germarium was found to be about 40 on average but was quite variable among individuals of a single genotype (32-51 over 25 germaria), as noted previously (Wang and Page-McCaw, 2018). At -6d and -5d the inferred number of ECs still to be made from dividing precursors was almost identical at 33 (19 r1 and 14 r2a) per germarium (Table 2). This approximates the number of adult ECs, consistent with the idea that all or almost all cells that will become adult ECs are still dividing at the start of pupation. The inferred number of ECs still to be made from dividing precursors dropped slightly at -4d (from 33 to 28) and more markedly by -3d (to 15) and -2d (to 13) (Table 2). We surmise that precursors of over half of the future adult EC population have ceased dividing by 2-3 days prior to eclosion. Moreover, the average number of dividing precursors for r1 ECs (4.7) was significantly lower than for r2a ECs (8.6) by -2d even though the total adult r1 EC population is higher (19 vs 14, inferred from -6d and -5d data). Thus, a reduction in precursor division appears to spread from the anterior towards the posterior as pupal development proceeds.

Low frequency clones to validate a common precursor for ECs and FSCs

The overall clone frequency (percentage of ovarioles with any marked cells in the germarium or early egg chambers) in the MARCM experiments tracing the fate of precursors marked from -6d to -2d was 60%, yielding an expectation that about 2/3 of marked ovarioles derive from marking a single precursor if all recombination events are independent and equally likely (see Methods). To obtain a lower frequency of marked clones, and hence a greater proportion deriving from a single cell, we used a multicolor marking strategy wherein a recombination event can lead to loss of GFP or a *lacZ* transgene, with or without RFP loss to yield six possible phenotypes (Reilein et al., 2017). Hence, for a given frequency of clone induction the proportion of a specific color combination will be substantially reduced. The two types of clone with the lowest frequency (because they require recombination at *FRT40A* and *FRT42B*) were GFP-only and *lacZ*-only, but we scored only the former because it was sometimes difficult to score all marked ECs for *lacZ*-only clones. GFP-only clones, induced at -5d and scored in newly-eclosed (0d) adults, were found at an overall frequency of 26/115 ovarioles so that an estimated 86%, calculated as for MARCM clones (see Methods), would be expected to derive from a single marked cell.

The patterns of GFP-only and other multicolor clones were very similar to those observed by MARCM analysis (Fig. 4). Among GFP-only clones that included FSCs, eight also included ECs and only two did not (Fig. 4B, C). We can therefore be confident that a single precursor at -5d can give rise

to both ECs and FSCs and that most FSCs originate from such precursors. The proportions (and yields) of GFP-only clone types were 42% EC-only (average 3.0 ECs), 31% EC/FSC (average 3.5 EC and 2.6 FSCs) and 8% FSC-only (average 4.0 FSCs) (Table 3).

Multicolor lineage tracing also showed clustering along the AP axis for individual GFP-only clones (Fig. 4A-C). Additionally, clones of different colors in the same germarium were generally offset along the AP axis. In some cases, the two clones likely derive from a single recombination event in a common parent, yielding "twin-spot" daughters (Fig. 4D-F). These observations graphically confirm the earlier conclusion that marked lineages spread a limited but significant distance along the AP axis (even for the two daughters of a cell undergoing recombination) and that the initially marked precursors have significantly different AP locations.

Follicle Cells produced during pupation derive from precursors that also yield FSCs and ECs

In the MARCM analysis presented earlier we inferred cell distributions in newly-eclosed adults from observations made 2d later in order to allow at least 4d for GFP marking to become clear. For MARCM clones induced early (at -5d) we were also able to examine newly-eclosed adults directly. This allowed us to score all marked FCs produced from precursors, as well as FSCs and ECs, because no egg chambers have matured beyond the point where FCs die and even the most recently produced FCs in region 2b of the adult germarium are readily distinguished from FSCs by Fas3 expression. From these data we can learn about the developmental origin of FCs, which are typically present surrounding two cysts in the germarium and four budded egg chambers in a newly-eclosed adult.

Most clones with marked FSCs also had marked ECs (24/27) (Fig. 5A, D), as observed in MARCM analysis at +2d and multicolor clone analysis, confirming a common precursor of ECs and FSCs. Almost all clones with marked FSCs also had marked FCs (25/27) (Fig. 5A), indicating a common precursor for adult FSCs and FCs. A significant proportion of all clones (23%) had marked ECs, FSCs and FCs, indicating that some individual pupal precursors give rise to all three cell types in newly-eclosed adults. Many ovarioles ("FC-only"; 25%) also contained marked FCs but no marked FSCs (Fig. 5C, D).

The locations of marked FCs were scored as "immediate" (region 2b), "germarial" (region 3) or in egg chambers ("ECh") 1-4 (occasionally three or five egg chambers were present). The percentage of clones with marked immediate FCs was higher for FSC/FC clones (56%) than for clones with marked FCs but no marked FSC ("FC-only") (16%). Conversely, the percentage of clones with marked FCs in at least one of the two terminal (most posterior) egg chambers was higher for FC-only clones (88%) than for FSC/FC clones (67%). Indeed, occupancy by marked FCs decreased gradually from anterior to

posterior for FSC/FC clones and with the opposite polarity for FC-only clones (Fig. 6A). Thus, derivatives of a given precursor were clustered along the AP axis in FSC/FC territory, as previously noted for EC/FSC territory. The idea that the fate of precursor derivatives is set largely by the AP position of precursors, with limited AP dispersal of derivatives, appears to be the governing principle all the way from the most anterior r1 EC derivatives to the most posterior FCs in newly-eclosed adults. Notably, while some clones contained only ECs or only FCs, clones with marked FSCs always contained ECs or FCs, indicating that there were no FSC-specific precursors at this time and that individual lineages regularly spanned the borders of adult cell identities.

Improved estimates of numbers of different precursor types just prior to pupation

Several ovarioles from animals heat-shocked 5d prior to eclosion contained marked FCs and marked ECs but no marked FSCs, strongly suggesting that these clones arose from two cells (because they were, unlike other clones, discontinuous). The frequency of such ovarioles (16%) was significantly higher than expected if all recombination events were independent (80% of ovarioles were predicted to contain single lineages because 67% of ovarioles contained no marked cells; see Methods). It is indeed possible that non-uniform temperature changes during heat-shock or other factors lead to some degree of clustering of recombination events rather than an even distribution among all ovarioles and all flies, especially when using mild heat-shock conditions to induce recombination events at a very low frequency. To account for the observed proportion of ovarioles with ECs and FCs we estimated that 30% of ovarioles with marked cells derive from a single marked cell (rather than 80% as estimated from the frequency of unmarked ovarioles), while the other 70% derive from exactly two marked cells. Based on this assumption, we calculated the component single cell clone frequencies and component cell numbers that would give rise to the scored raw data (see Methods). With this revision, the estimated number of precursors just prior to pupariation (see below) for precursors giving rise only to ECs (15.1), to EC and FSCs (with or without FCs) (3.1), only FSCs (with or without FCs) (1.2) or only FCs (4.6) totaled about 24 (Fig. 5E; Table 3). The number of TJ-positive cells counted in pupal ovaries at 12h APF was 38, roughly consistent with the revised estimates from lineage analysis.

Multicolor GFP-only clones were used previously to provide the most definitive evidence that an individual precursor cell can produce both adult ECs and FSCs; we cited an expected frequency of 86% of marked ovarioles deriving from a single cell if recombination events were random and independent (77% had no marked cell). The observation that 42% of marked ovarioles included only ECs while 8% included marked ECs and FCs suggests that a slightly lower proportion of ovarioles harbor single-cell lineages. If we assume that only 70% of ovarioles with marked cells derive from a single cell, with the

remaining 30% deriving from two cells (likely a small overestimate of double-clones) we can calculate the component single cell lineage frequencies and component cell numbers that would give rise to the scored raw data, as above (see Methods). With this revision, we still find evidence that a single precursor cell gives rise to both ECs and FSCs (25% of all marked lineages) and that the frequency of such precursors greatly exceeds precursors that produce FSCs but no ECs (10%). The deduced proportions of clone types and the number of precursors of each type (9.0 EC, 4.2 EC/FSC, 1.6 FSC, 2.4 FC and 17 total precursors) are similar to those calculated above from the similarly timed MARCM experiment (Fig. 5E; Table 3).

We used the same methods to estimate single-cell lineage types and yields from a MARCM analysis of clones induced 3.5d prior to eclosion. Here the proportion of labeled ovarioles (94%) and of EC/FC clones was particularly high, probably because there are many more dividing precursors than at -5d, so the deduction of single cell lineage content is likely less reliable. In both the raw data and derived lineage types it was clear that the proportion of FC-restricted lineages was much higher than at earlier times, while marked FSCs were still mostly accompanied by marked ECs, consistent with our earlier analyses of MARCM clones analyzed in in 2d-old adults. We estimated that the proportions of single-cell lineage types were EC-only (51%), EC/FSC(/FC) (7%), FSC(/FC) (4%), FC-only (38%) and that the total number of dividing precursors was about 35 (Fig. 5E; Table 3). Based on earlier analysis of MARCM lineages induced at -4d and -3d and examined at +2d, there should be between 5 and 18 non-dividing precursors (say 11.5) at -3.5d (Table 2). Thus, we estimate that there are 13.3 FC-only precursors within a total precursor population of 46.4 (29%) at this time (corresponding to 36h APF; see later).

FC founders per egg chamber and timing of FC recruitment to first egg chamber

During adult oogenesis, an FC is defined by continued association with a germline cyst. The first FCs are permanently recruited to germarial stage 2b cysts and it has been estimated that there are on average 5-6 founder FCs per cyst (Reilein et al., 2017; Reilein et al., 2018b). The number of founders can be determined by measuring the fractional contribution of a single founder to the whole FC epithelium around a single egg chamber. However, marked lineages induced in precursors to founder FCs will sometimes first divide and then contribute more than one founder FC to a given egg chamber. We examined the distribution of marked FC contributions from FC-only precursors during pupation in order to gain insight into the number of founder FCs seeding each egg chamber and the time at which founder FCs were first restricted to populating only the first budded egg chamber.

When plotted in bins of 3% for clones induced at -5d, the distribution of marked cells as a percentage of an entire egg chamber FC epithelium are clustered around 9-12% (a peak with a central cavity) and 24-27% (Fig. 6B). The distribution observed from a similar analysis of clones induced at 3.5d before eclosion was extremely similar (Fig. 6D). We do not expect to observe sharp peaks in the distribution of FC contributions because each founder FC may subsequently divide a different number of times; in particular, polar and stalk cells cease division much earlier than remaining FCs (Margolis and Spradling, 1995; Tworoger et al., 1999), likely accounting for the high representation of contributions from 0-6%. The values clustered around 9-12% and 24-27% plausibly correspond to the most common contributions of a single founder cell and two founder cells, respectively. If we consider only FC contributions lower than 25.5% (the mid-point of the second peak) we will most likely include the majority of clones deriving from single FC founders and only a small number of clones deriving from two or more marked FCs; this subset can give an approximation (likely a modest overestimate) of the contribution from a single founder FC. Within this restricted sample, the average contribution over all egg chambers in newly-eclosed adults was 12.2% (33 FC patches) for -5d clones and 12.4% (43 FC patches) for -3.5d clones, suggesting an average of at least eight FC founders per egg chamber. Considering only the terminal egg chamber, average FC occupancy was 12.2% for -5d clones and 11.9% for -3.5d clones, almost identical to the overall average.

To determine when FCs were first allocated to the most mature germline cyst during pupation we looked at the distribution of FC-only clones amongst egg chambers. For clones induced 5d before eclosion there were fifteen ovarioles with marked FCs in the most posterior egg chamber. Twelve of these also had marked FCs in more anterior regions, mostly occupying at least two additional egg chambers. Hence, FC precursors were not yet constrained to contribute to a single egg chamber. The distribution of FCs from FC-only clones induced 3.5d before eclosion was more restricted; 21 of 34 ovarioles with labeled FCs in the terminal egg chamber had no other labeled FCs (Fig. 6E, F). The 13 exceptions all had marked FCs in egg chamber 3 (Fig. 6E, G) and are too many to be explained by the presence of two lineages. In most ovarioles with marked FCs in egg chambers 3 and 4 (9/13) the FC contribution to egg chamber 4 is less than 25.5%, suggesting that the initially labeled precursor at 36h APF generally divided one time before one daughter became an FC founder for egg chamber 4 and the other later contributed to egg chamber 3. In the majority of ovarioles with only egg chamber 4 labeled (12/21), marked FCs occupied more than 25.5% of the epithelium, suggesting that in most cases the initially labeled precursor divided before contributing two founder FCs to egg chamber 4. Thus, it appears that founder FCs were fully allocated to the first-produced egg chamber roughly one cell cycle after 36h APF, by which time many of the first founders allocated had already divided. We do not know the cell cycle length for these FC-only precursors but expect (from lineage amplification data) that it is

shorter than 24h and may be close to 11h, the estimated cycling time for early FCs in adult ovarioles (Margolis and Spradling, 1995).

Marked FCs occupied only the two terminal egg chambers (one or both) in 36 out of 52 ovarioles with FC-only clones induced -3.5d before eclosion (Fig. 6E). Marked FCs occupied only territory anterior to the two terminal egg chambers in six ovarioles. Some or all of the remaining 10 ovarioles with hybrid patterns plausibly harbor two FC-only lineages. Thus, by 36h APF the FC-only precursors appear to be segregated into two populations with the majority (roughly 46/62, or over 70%, if we consider the 10 hybrid patterns to contain one lineage of each type) contributing only to the two terminal egg chambers and other precursors contributing only to more anterior egg chambers. Ovarioles that include marked FSCs only rarely contributed to the two terminal egg chambers (Fig. 6C). Indeed, the few exceptions may well derive from ovarioles that harbor an FC-only lineage (53% frequency overall) in addition to an FSC-containing lineage (26% overall). Thus, at 36h APF (see below), it appears that over two-thirds of FC-only precursors are constrained to contribute to one or both of the first two egg chambers, while more anterior egg chambers are later populated by a combination of FC-only and FSC/FC precursors. It is likely that all FCs contributed to the two terminal egg chambers derive from FC-only precursors.

Integration of cell lineage and morphological evidence

In our cell lineage studies a “-5d sample” was generated by collecting very young adults (less than a 6h range) centered around 120h after heat-shock. The time between puparium formation and eclosion was generally a few hours less for these adults than for animals used in morphological studies but there is also a short delay between heat-shock and genetic marking of a cell. (Golic and Lindquist, 1989). Consequently, the time a marked cell is born in a “-5d sample” likely corresponds closely to puparium formation, consistent with the observed labeling of some Cap Cells but very few TF cells, which have ceased division by that stage. In our morphological studies, samples were initially collected relative to directly observed larval immobility of each animal analyzed. After this initial calibration we were able to determine pupal stage according to ovary morphology.

Lineage data suggested that some precursor lineages are restricted to the most advanced germline cyst at 36h APF (-3.5d), with the remainder following one division cycle later. By 48h APF, all germaria have a single cyst in the most posterior region (Fig. 2) but neighboring somatic cells only express very low levels of Fas3 (Fig. 7D). In adult germaria, even the most recently recruited FCs surrounding a stage 2b cyst express high levels of Fas3; a subset of those cells must then become specialized polar and stalk cells before the egg chamber can bud about 24h later. The ICs described

above that are just starting to express Fas3 at 48h APF therefore appear to be far behind schedule, given that the first egg chamber will bud at about 56h APF on average (Fig. 1). These observations pose the question of whether these ICs are indeed the cells that will form the FCs of the first budded egg chamber.

An Extra-Germarial Crown (EGC) forms prior to egg chamber budding

Posterior to the intermingled germline cells and somatic ICs of the germarium are somatic cells with strong Fas3 staining at 24h APF onward (Fig. 1; Fig. 7B). These have all previously been considered as progenitors of basal stalk cells and indeed most can be seen to be intercalating into a stalk structure from 36h APF onwards (Fig.1; Fig. 7), as previously described (Godt and Laski, 1995; Vlachos et al., 2015). However, we noticed that the most anterior of these Fas3-positive cells express TJ and form a small multi-layered cone or crown around the posterior of the developing germarium that is quite prominent by 48h APF (Fig. 7A-D). We refer to those TJ/Fas3-positive cells posterior to the single layer surrounding the most posterior germline cyst as the Extra-Germarial Crown (EGC). A smaller number of similarly situated TJ-positive EGC cells can be seen at earlier times (Fig. 7A-D, H). A population of cells that expresses both TJ and Fas3 strongly is notable because there is evidence from manipulation of TJ activity in adult ovaries that TJ generally represses Fas3 expression (Li et al., 2003), while a principal characteristic that distinguishes adult FCs from other TJ-expressing cells (FSCs and ECs) is strong Fas3 expression (Reilein et al., 2017). Key questions, which we address below, are therefore whether the most posterior ICs with low Fas3 expression at 48h APF become the FCs of the first-produced egg chamber and what becomes of the newly-identified group of EGC cells.

A stage 3 germline cyst is initially separated from the posterior egg chamber by only a small number of somatic cells just prior to budding from an adult germarium. During budding, the cyst remains associated with adjacent somatic FCs, which emerge as a monolayer epithelium connected to the germarium by a thin, short stalk of specialized cells. By contrast, prior to budding of the first pupal egg chamber there is a large accumulation of somatic EGC cells posterior to the germarium and after budding, the first egg chamber is often found much further from the germarium than in adults (Fig. 1H). The intervening space is occupied by partially intercalated TJ/Fas3-positive cells and by a small “secondary” EGC, crowning the germarium (Fig. 7G). In samples with two budded egg chambers (72-84h APF) or more, the newly budded egg chamber is close to the germarium (Fig. 1I), resembling adult ovarioles. Thus, formation of the first egg chamber involves a morphological process quite different from in adults; this is partly recapitulated by the second egg chamber before adopting a typical adult morphology.

Live imaging reveals EGC cells as a source of FCs for the first egg chamber

We adapted a live imaging protocol previously developed for adult ovarioles (Reilein et al., 2018a) in order to view pupal ovaries and track individual somatic cells. We were able to follow isolated live ovaries for up to 15h, during which time many cell movements and cell divisions were observed, suggestive of continued normal behavior. We first used samples where all cells were labeled by expression of a *ubi-GFP* transgene. Later, we used animals with multicolor clones induced 2-3d earlier, so that some cells had lost either GFP or RFP expression. Variability in the levels of GFP and RFP simplified the task of following individual cells over time.

From 30h APF a variety of tracked ICs mostly maintained their relative AP locations within the developing germarium but with a few exceptions (the cyan cell moved anterior to the pink cell in Fig. 8A). From 40h APF one of two similarly placed germline cysts adopts the most posterior position in the germarium while somatic ICs appear to move independently of the cysts (the shaded white cyst moved past the pink and white cells in Fig. 8B).

Imaging of an ovary from 48h APF onwards captured the key process of egg chamber budding for the first time (Fig. 9; Fig. S2, S3; Movie S1). The most posterior germline cyst moved away from the germarium into EGC territory, as EGC cells enveloped the cyst. The cyan cell started within the EGC, contacted the cyst prior to 8.3h and remained associated for the next 6.5h (Fig. 9; Fig. S3). The white cell, which initially lay posterior to the morphologically defined EGC and initially (from comparison to fixed images) likely does not have strong TJ expression, entered EGC territory within 4h and became associated with the germline cyst by 12h (Fig. 9; Fig. S3). The magenta cell, initially just posterior to the cyst, moved to the midpoint of the budded egg chamber (Fig. 9; Fig. S2C). The red cell, which started a little further anterior, and would be considered an IC, maintained contact with the posterior-moving cyst and was last seen at the anterior aspect of that cyst, leaving ambiguous whether it remained associated or moved past the cyst to await the second cyst to bud (Fig. 9; Fig. S2C). The yellow cell in the germarium above started from a similar location but ended up anterior to the budded cyst, forming part of a secondary EGC just beyond the germarium (Fig. 9; Fig. S2B). Thus, over the nearly 15h of live imaging the newly-budded cyst acquired a set of closely-associated cells of epithelial appearance that derived from the EGC region, slightly posterior to the EGC region and the extreme posterior of the germarium at 48h APF. Imaging of later stages (below) suggests that some of the cells surrounding the budding cyst may be moving stochastically with an anterior trend, so it seems possible that cells initially derived from the germarium may end up anterior to the first budded egg chamber but most cells derived from the EGC, which are further posterior, likely remain on the budded cyst.

Imaging from about 60h APF, cells on the first budded egg chamber were seen to move anterior and lose contact (Fig. S4A). The most posterior cyst in the germarium of the same ovary rounded up and started to move into the secondary EGC, which included dividing cells (Fig. S4B, C). ICs anterior to that cyst moved further posterior as the germarium elongated and mostly appear poised to associate with later cysts (Fig. S4C).

In summary from all live imaging spanning 30h-68h APF, it seems likely that all TJ-positive cells observed in fixed samples (Fig. 7) retain TJ expression and become one of the adult TJ-expressing cell types, ECs, FSCs or FCs. Furthermore, the FCs surrounding the most mature egg chamber in newly-eclosed adults appear to derive solely or principally from the Extra-Germarial Crown of somatic cells that accumulates between 12h and 56h APF. The ICs that express Fas3 weakly at 48h APF probably contribute principally to the second, third or even later egg chambers formed during pupation, although it remains possible that some of the most posterior ICs may also associate with one of the first two cysts to bud.

Live imaging also afforded information about cell movements within the germarium, revealing apparently stochastic movements in all directions that sometimes altered the spacing of pairs of cells along the AP axis. These observations are consistent with the deductions from lineage analysis that somatic cells tend to remain in the same relative AP positions over a period but that a group of sister cells can spread over the AP axis.

Pattern of precursor divisions along the AP axis

The analysis of MARCM clones in 2d-old adults provided average numbers for the yield of ECs and FSCs per precursor of each type starting at different times from 6d to 2d before eclosion (Table 1). The proportion of dividing precursors of each type is also indicated by the frequency of different clone types. From these data it is clear that there is a severe reduction in EC-only precursor division rates from -4d to -2d (24h to 72h APF) with the frequency of such clones falling from 58% and 57% at -5d and -4d to 30% at -3d and 14% at -2d. Moreover, among EC-only precursors the decline in division spreads from the anterior; the yield of r1 ECs relative to r2a ECs declines from 2.2 (-5d) and 2.6 (-4d) to 0.9 (-3d) and 0.8 (-2d). The yield per EC/FSC and FSC precursor is consistently higher than for EC-only precursors at all times of clone induction, indicating higher division rates in more posterior locations. These yields do not include FCs and therefore account for only a fraction of EC/FSC and FSC precursor output, precluding numerical assessment of whether the increasing proliferation gradient from r1 ECs through EC/FSC precursors extends further posterior.

We incubated dissected pupal ovaries at various developmental stages with EdU in vitro over a 1h time period to detect cells in S phase. From 0-24h APF ICs throughout the germarium often incorporated EdU (Fg. S1A-C). By 48h APF, the prevalence of anterior EdU-labeled cells was quite low, with EGCs, by contrast, exhibiting frequent EdU signals (Fig. S1D). Even at 60h APF, however, an occasional IC in the anterior half of the germarium could be found with EdU label; none were evident at 96h APF (Fig. S1E, F). At 96h APF some cells anterior to strong Fas3 expression, which may be r2a EC or EC/FSC precursors, did still incorporate EdU.

We also used the FLY-FUCCI system to measure cell cycling. In this system, RFP- and GFP-tagged proteins accumulate during the cell cycle under the influence of a chosen promoter, while degrons from CycB and E2F1 promote rapid degradation of RFP and GFP fusion proteins at the start of G1 and S phase, respectively (Zielke et al., 2014). While RFP and GFP are expected to be reliably absent during G1 and S phase, respectively, the speed of recovery of each signal during the next phase of the cell cycle depends on the strength of transcription of FLY-FUCCI components. We used *UAS*-driven *FLY-FUCCI* transgenes and found *C587-GAL4* to be more effective than *tj-GAL4* or *act-GAL4* in producing GFP and RFP FUCCI signals in the developing somatic IC population.

In adult germaria all r1 ECs express only GFP (Fig. 10G), indicating G1 (or a G0 state). r2a ECs are a mix of GFP-only G1 cells and cells with both GFP and RFP, indicating G2 (Fig. 10G). FSCs additionally include some cells with RFP-only (late S-phase) and no GFP or RFP (early S-phase, verified by co-labeling with EdU) (D. Melamed pers. comm.). From 12-36h APF ICs at all AP locations in the germarium included some cells with each FUCCI color combination, although G1 cells were always most frequent in more anterior regions (Fig. 10A-D). By 48h APF almost all somatic cells in the anterior half of the germarium were in G1 or G0, consistent with substantially reduced cycling (Fig. 10E). A large fraction of EGC cells were in S phase (marked by RFP only), in contrast to nearby basal stalk cells (Fig. 10E'). By 96h APF, after two or three egg chambers have budded, the *C587*-expressing domain has retracted anteriorly, roughly to territory anterior to strong Fas3 staining and the pattern of FUCCI labels is quite similar to adults, with anterior cells uniformly in a G1 or G0 state, followed by cells largely in G1 and G2 and then some cells in S phase also (Fig. 10F). Thus, direct observation of EdU incorporation and cell cycle markers confirms the progressive decline in anterior IC proliferation over time that was inferred from lineage analyses and suggests that the anterior to posterior gradient of proliferation stretches all the way to posterior ICs and EGC cells, which appear to cycle rapidly.

A putative FSC precursor marker yields lineages that also produce ECs and FCs

Recent single cell RNA sequencing of developing ovaries in late third instar larvae led to the discovery of a variety of genes with regional expression patterns (Slaidina et al., 2020). A set of GAL4 drivers, which partially reproduced the expression patterns of selected parent region-specific genes, were used in lineage tracing experiments to determine precursor-product relationships. A *bond-GAL4* driver was used together with a temperature-sensitive *GAL80* transgene to initiate GFP-marked lineages using standard G-trace reagents (Evans et al., 2009), keeping animals at 29C during larval stages, switching to 18C about one day after pupariation and scoring marked cells in 2d-old adults (Slaidina et al., 2020). Most of the labeled ovarioles (31/32) included marked FSCs (inferred from the presence of early marked FCs) or FCs (the fraction with FSCs was not explicitly documented) and over half of these (19/31; one has only marked ECs) also contained marked ECs. We used the same reagents to compare outcomes directly with our timed lineage studies that target all dividing precursors, scoring results in newly-eclosed adults so we could clearly resolve FSCs and FCs that are directly produced from precursors.

We found a high frequency of marked cells when animals were kept at 18C throughout (37 labeled ovarioles out of 108) with marked ECs and FSCs present in almost all cases (35/37) (Fig. 11A-C). We saw no increase in the proportion of ovarioles with marked ECs or FSCs when larvae were raised at 29C and moved to 18C about 2d after pupariation (eclosing 6d later; 13 of 44 ovarioles labeled) or when animals were raised at 18C before shifting to 29C for the final 3d or 4d of pupation (23 of 88 ovarioles labeled) (Fig. 11D). In all cases the observed clones were dependent on *bond-GAL4* (a much lower frequency of marked lineages, with different patterns of marked cells, was observed in parallel experiments with a *Con-GAL4* driver). Because we observed no marked temperature dependence for these EC/FSC-containing clones we cannot define the time at which cells were first marked. However, we expect that most lineages were initiated close to the larval/pupal transition based on the lineages themselves, as described below.

The marked lineages were similar (Fig. 11A-D) to those we described earlier using *hs-flp* to initiate clones at pupariation (5d before eclosion), suggesting that they had been induced at a similar time. The majority of ovarioles from the *bond-GAL4* experiments (considering all three temperature conditions together) included either only marked ECs (about 40%) or marked ECs and FSCs (about 50%, almost all together with FCs) (Fig. 11D). Only one out of 73 labeled ovarioles had marked FSCs but no marked ECs; that ovariole also included marked FCs. The number of labeled ECs and FSCs (when present) per germarium was consistently higher than we observed with *hs-flp* induced clones induced at pupariation (Fig. 11A-C; Table 3). Thus, if the two sets of clones were initiated at similar

times most labeled ovarioles in the *bond-GAL4* experiment must contain lineages derived from more than one precursor. We therefore derived the component single clone types (frequency and number of products) that would produce the observed *bond-GAL4* > *G-trace* results if we assume that every ovariole has exactly two marked lineages (roughly accounting for the increased cell numbers seen; see Methods). The results are remarkably similar to the single clone types and content deduced for *hs-flp* induced clones 5d prior to eclosion, (Fig. 11E; Table 3). The most significant differences were a greater yield of ECs per EC-only lineage and fewer FC-only lineages, consistent with slightly earlier clone initiation in the *bond-GAL4* experiments. It is therefore plausible (though not the only possible explanation of the primary data) that *bond-GAL4* labeled precursors sporadically throughout the IC region shortly before pupariation. Consequently, in keeping with results from MARCM studies, the observed FSC-containing lineages and those inferred to derive from a single cell also included ECs in almost all cases (as well as FCs). Our results do not support the labeling by *bond-GAL4* of a precursor that is specific to FSCs and not ECs.

bond gene expression was described as being patchy but distributed among all ICs at early third instar before concentrating in a region just posterior to the IC domain (Slaidina et al., 2020). The results described above are consistent with *bond-GAL4* driven clone initiation in the former pattern. Our live imaging studies suggest that cells in the latter, posterior location may contribute to the EGC by 36-48h APF and then to FCs of the first budded egg chamber. When animals with *bond-GAL4* and *G-trace* were maintained at 29C during the last 3d or 4d of pupation we observed an additional type of lineage, either in isolation or together with the types of marked cells described above (55/88 ovarioles; 0/108 when at 18C throughout) (Fig. 11G). Here, a few isolated FCs or small clusters in the most mature egg chamber, and no others, were labeled, suggesting several independent recently initiated lineages. Some of the GFP-labeled FCs also expressed *UAS-RFP*, indicating current or recent *bond-GAL4* activity (Fig. 11G). Surprisingly, the same type of clone was observed if animals moved from 29C to 18C about 2d after pupariation (30/44 ovarioles, with only 6 ovarioles also including RFP-expressing FCs) (Fig. 11F), suggesting that some of the FC-only clones confined to the first budded egg chamber may originate from posterior EGC cells prior to budding of the first egg chamber.

Evolution of the pattern of Wnt pathway activity in the FSC niche

Wnt pathway activity in adult germaria, measured with a Fz3-RFP reporter, declines from a high-level in r2a ECs to zero in the earliest FCs (Fig. 12I, L) (Reilein et al., 2017; Wang and Page-McCaw, 2014). Genetic manipulations that increased Wnt pathway activity in an adult FSC autonomously resulted in a more anterior location with eventual conversion of all such FSCs to ECs,

while genetic loss of Wnt pathway activity autonomously reduced EC production and caused FSCs to accumulate in the most posterior layer of the normal FSC domain (Reilein et al., 2017). The sources of Wnt in the adult germarium include high levels of Wg and Wnt6 production in Cap cells and lower levels of Wnt 2 and Wnt4 in ECs (Forbes et al., 1996; Luo et al., 2007; Sahai-Hernandez and Nystul, 2013; Upadhyay et al., 2018; Waghmare and Page-McCaw, 2018; Wang and Page-McCaw, 2018).

In pupal germaria Fz3-RFP was first detected 27h APF and showed a marked increase in intensity between 36h and 48h (Fig. 12B-G, J). At all stages Fz3-RFP was higher in anterior than posterior regions, consistent with the possibility that Cap Cells, which are specified at the anterior of the germarium very close to the start of pupation, and even developing EC precursors, may be major sources of Wnt ligand, as in the adult. At 48h APF the decline in Fz3-RFP was spread over the posterior two-thirds of the germarium (Fig. 12 G, J). By 60h APF the domain of consistently high Fz3-RFP expression occupied a larger anterior territory, extending roughly halfway to the region of strong Fas3 expression, followed by a steeper decline to background levels (Fig. 12H, K). At all stages, the border of strong Fas3 expression coincided with very low levels of Wnt pathway reporter activity, suggesting the possibility that Wnt signaling may inhibit Fas3 expression.

Influence of Wnt pathway activity on precursor behavior

To determine the influence of Wnt pathway activity on the behavior of individual precursors during pupal development we repeated MARCM lineage studies with the recombination event that marks cells simultaneously creating a homozygous mutation that either inactivates (null *arr* mutation) or hyperactivates (strong *axn* or *apc1 apc2* double mutation) the Wnt pathway. We performed two sets of experiments with *arr* mutations and one each for *axn* and *apc1 apc2*, inducing clones at 2-6d before eclosion and examining ovarioles in 2d-old adults. Outcomes were similar for each pair of tests, so we aggregated the results for the two experiments with reduced Wnt pathway activity (*arr*), the two with increased activity (*axn*, *apc*), and three controls (Fig. 13A-F).

Loss of *arr* activity consistently led to a decreased frequency of EC production relative to FSCs, while increased Wnt pathway activity produced the opposite outcome. Thus, the percentage of all cells in marked clones that were FSCs was, on average from -6d to -2d, 42% for controls, 61% for *arr* and only 20% for *axn*/*apc*, with the same trend evident for each time-point (Fig. 13C). The proportion of all clonal derivatives that become r1 ECs was consistently lower than controls for *arr* mutant precursors at all times of clone induction from -6d to -2d (average 13% vs 32%) (Fig. 13A, D, E). By contrast, the proportion of r2a ECs was markedly lower for *arr* mutant precursors than controls only when clones were induced at -2d (Fig. 13B). These results suggest that loss of Wnt pathway activity results in

posterior movement of precursors relative to wild-type neighbors at all times from -6d onward. At early stages this results in r1-only precursors transforming to r2a and FSC-producing locations. At intermediate times the increase of r2a precursors from r1 precursors is offset by conversion of r2a precursors to FSC fates, while in the last stages there is a net deficit in r2a EC production because the majority of actively dividing precursors are in regions that can only produce r2a ECs or FSCs (and FSC fate is favored by loss of Wnt pathway activity). Thus, normal Wnt pathway activity is important for limiting posterior movement of precursors over a wide domain throughout pupal ovary development.

Increased Wnt pathway activity consistently increased the proportion of r2a ECs in clones induced from -6d to -2d, while the proportion of FSCs was reduced (Fig. 13B, C, D, F). These results suggest that cells with increased Wnt pathway activity adopt more anterior positions within the domains that normally give rise to either ECs or FSCs. The proportion of r1 ECs produced by *axn/apc* mutants was almost identical to controls for the entire -6d to -2d induction period (Fig. 13A). Thus, the reduced levels of Wnt pathway activity observed in posterior regions of normal germaria that include EC/FSC and FSC precursors, is important for maintaining a sufficiently posterior location to become an adult FSC.

It is not straightforward to measure the effect of altered Wnt pathway activity on precursor division rates from lineage data for a number of reasons. First, the cellular yield per clone is dependent on clone induction frequencies, which can be quite variable even within a single experiment. Second, alteration of cell locations will affect yields because more anterior cells cease division earlier. Third, the yield of FCs cannot be scored (and will likely differ for mutations affecting AP location). Notwithstanding these reservations, the average number of cells in clones with altered Wnt pathway activity was quite similar to controls (4.8 cells per clone for controls, 3.6 for *arr* and 5.4 for *axn/apc* on average for -6d to -2d clones), suggesting that there was no drastic change in the rate of precursor division over most of pupal development. In adults, excessive Wnt pathway activity was found to reduce FSC division rate significantly, while loss of Wnt pathway activity had little effect.

We also induced MARCM clones with increased (*axn* mutation) or decreased Wnt activity (expression of dominant-negative TCF (van de Wetering et al., 2002)) at -5d and examined ovarioles in newly-eclosed adults, allowing us to measure the production of FCs in addition to ECs and FSCs. Similar to the observations made for clones examined in 2d-old adults, increased Wnt signaling resulted in a loss of marked FSCs, an increase in marked r2a cells and no change in the proportion of marked cells in region 1 (Fig. 13G). Also, reduced Wnt signaling led to reduced production of r1 ECs and an increase in the proportion of r2a ECs (Fig. 13G, I, J). However, there was no increase in the proportion of marked FSCs, contrasting with results seen for *arr* mutations; that is likely because dominant-negative TCF produced a lesser reduction in Wnt pathway activity.

The effect of genetically altered Wnt pathway activity on FC production was assessed from the distribution of clone types in newly-eclosed adults. Increased Wnt pathway activity reduced the frequency of clones with FCs but no FSC (from 26% to 2%) and the total frequency of clones that included marked FCs (from 51% to 5%) (Fig.13H). Reduced Wnt pathway activity did not have a large effect on the frequency of clones with FCs but no FSC (19% vs control 26%) or the total frequency of clones that included marked FCs (41% vs control 51%), reducing both proportions.

The effect of altering Wnt pathway activity on the distribution of EC and FSC clone types was in accord with results described above from counting total production of r1 and r2a ECs and FSCs summed over all clones. Thus, increased Wnt activity resulted in a greater frequency of clones with ECs but no FSCs (91% vs 63% in controls) and a lower frequency of clones with FSCs (7% vs 28% in controls) but with little change in the frequency of clones with marked r1 ECs (82% vs 78% in controls). Wnt pathway reduction slightly reduced the proportion of clones containing r1 ECs (from 78% to 67%); it did not reduce the frequency of clones with ECs but no FSCs (63% vs 63% in controls) or increase the proportion of clones with marked FSCs (26% vs 28% in controls).

Thus, increased Wnt pathway activity increased EC production (but not r1 EC production) and drastically decreased both FSC and FC production. Both reducing and eliminating Wnt pathway activity reduced r1 EC production but only loss of pathway activity reduced FSC production.

Influence of JAK-STAT pathway activity on precursor behavior

JAK-STAT pathway activity in adult germaria, measured by a reporter containing multiple STAT binding sites (*stat-GFP*) is graded from posterior to anterior over the FSC domain, with ligand emanating principally from polar follicle cells, which first differentiate shortly before egg chamber budding (Bach et al., 2007; Vied et al., 2012). Loss of JAK-STAT activity has been reported as greatly reducing FSC proliferation, while excess JAK-STAT activity has the opposite effect (Vied et al., 2012). Additional roles of JAK-STAT signaling in adult FSCs are currently under investigation.

In pupal germaria, *stat-GFP* expression was detected only at very low or background levels at early stages (Fig. S5A). A clear signal was first evident in a graded pattern declining from the posterior of the germarium at 60h and that pattern was maintained with increasing intensity thereafter (Fig. S5B-D). The onset of this pattern is shortly after the first egg chamber buds and therefore consistent with ligand production from polar cells, as in the adult. Within egg chambers *stat-GFP* expression was strongest adjacent to polar cells. To determine when polar cells form, we stained ovaries with Castor. In adults Castor is initially expressed in all early FCs but is then lost in all FCs other than polar and stalk

cells (Dai et al., 2017). We found Castor was confined to polar and stalk cells after the first egg chamber budded (Fig. S5E).

We manipulated JAK-STAT pathway activity in MARCM clones induced by heat-shock 5d before eclosion and examined marked lineages in newly-eclosed adults. Loss of *stat* activity resulted in a distribution of clonal derivatives very similar to that described for *axn* mutations (Fig. 13K). Thus, the fraction of all labeled cells that were FSCs was greatly reduced (6% vs 30% control) but the fraction of cells that were r1 ECs was unchanged (49% vs 51% control) (Fig. 13G). Accordingly, the proportion of clones that included FSCs was reduced (6% vs 28% control), the proportion of clones with ECs but no FSCs was increased (from 63% to 91%) and the proportion of clones with r1 ECs was not increased (70% vs 78% control). Loss of stat activity also reduced the frequency of clones with FCs but no FSC (from 26% to 6%) and the total frequency of clones that included marked FCs (from 51% to 8%) (Fig. 13H). Thus, in the absence of JAK-STAT activity we deduce that more posterior precursors, which would otherwise give rise to FSCs and FCs moved significantly anterior at some stage(s) during pupal development. The average size of clones was not significantly altered for the two major clone categories: clones with ECs but no FSCs (336/129=2.6 vs 156/62=2.5 control) and clones with ECs and FSCs (68/9=7.6 vs 194/24=8.1 control), suggesting that loss of *stat* activity does not greatly alter division rates in anterior regions through most of pupation. The consequences in more posterior regions are largely unknown because stat mutant cells mostly moved out of these regions and because we cannot count the number of FCs produced by posterior cells in order to measure division rates accurately.

Increased JAK-STAT activity due to expression of excess JAK (*UAS-Hop*) resulted in a large increase in clone size, with many marked cells throughout the germarium (Fig. 13L, M). Also, there was ectopic Fas3 expression in marked cells anterior to the normal Fas3 border (Fig. 13L) and some germaria had distorted morphologies, precluding reliable scoring of cell types. Clearly the proliferation of pupal IC cells can be stimulated significantly by artificially increasing JAK-STAT activity.

Discussion

An important general objective, exemplified here by FSCs, is to describe the origin of adult stem cells and surrounding niche cells and understand how the number and organization of these cells is instructed during development. Our investigations of changing morphology, key marker expression and cell lineage reveal a gradual and flexible adoption of cell types according to AP location throughout pupal development, rather than a series of discrete definitive cell fate decisions (Fig. 14). Thus, adult EC niche cells and FSCs develop from a common group of dividing precursors (ICs) interspersed with developing germline cysts and starting immediately posterior to Cap Cells, which serve as adult niche cells for both GSCs and FSCs, and are already specified by the start of pupation. The most anterior ICs become r1 and r2a ECs and markedly attenuate division, starting from the most anterior locations, during the second half of pupation (Fig. 14). More posterior ICs initially produce both ECs (mainly r2a) and FSCs but over time their most posterior descendants no longer produce ECs; most produce FSCs and FCs, while the most posterior produce only FCs. A subset of FC precursors accumulates beyond the interspersed somatic and germline cells of the developing germarium during the first two days after pupariation to form a newly-recognized structure that we termed an Extra-Germarial Crown (EGC) (see 48h APF in Fig. 14). These cells receive and then envelop the most mature germline cyst as it migrates out of the germarium in a remarkable morphological process of egg chamber formation that is quite different from egg chamber budding in adults. Soon after the formation of the first two egg chambers the morphology and marker gene expression pattern of the germarium resemble those of adult germaria, likely in response to establishment of a key niche signaling emanating from newly-differentiated polar FCs in budded egg chambers.

EC, FSC and FC precursors might in principle adopt fate-appropriate AP locations during pupation stochastically or they might be guided by memory of an early-instructed fate, by selective adhesive interactions with germline cysts of differing maturity or in response to potentially longer-range extracellular signals. We found that the fate of developing precursors was drastically altered by genetic manipulation of Wnt and JAK-STAT signaling pathways. Altered Wnt signaling affected fate outcomes across the whole domain from anterior EC to FC precursors and throughout pupation, with higher Wnt signaling resulting in movement to more anterior locations. Loss of JAK-STAT pathway activity had a similar consequence to elevated Wnt pathway activity but the critical relevant times were not established. Elevated JAK-STAT activity greatly stimulated precursor proliferation, unlike the other manipulations of JAK-STAT and Wnt pathways, precluding analysis of any potential effects on

precursor cell fates. Both Wnt and JAK-STAT pathways showed graded distributions, of opposite polarity and different times of inception, across the IC precursor region.

Identity, location and numbers of EC, FSC and FC precursors through pupal development

This study is the first to examine ovary development during pupal development through lineage analyses initiated at different times or by systematic analysis of fixed specimens and live imaging. Each approach included some challenges and leaves some issues unresolved but several key findings were conclusive and supported by all three approaches.

It is systematically challenging to conduct lineage analyses where only a single precursor is labeled in each developing ovariole because the number of dividing precursors that can potentially be labeled is large (more than 20 even at the earliest stages). This challenge was addressed by using very mild heat-shocks to initiate clones through *hs-flp* induction, a multicolor labeling technique that reduces the frequency of a specific color combination substantially relative to single-color clones, and by using information about clone frequencies and direct indications of composite clones to derive estimations of strictly single-cell lineage frequencies and yields. The results led to robust conclusions that many precursors at the start of pupation yield only ECs, a smaller proportion yield both ECs and FSCs (as well as FCs) and very few produce FSCs with no ECs. Common precursors for ECs and FSCs persist for at least the first 72h of pupation (later times were not tested), although they are exceeded in number by 72h APF by precursors that produce FSCs but not ECs. All such FSC lineages also included marked FCs in newly-eclosed adults. Thus, there is no cell or group of cells specifically assigned over this period to produce only FSCs or all FSCs.

The most distinctive group of precursors gives rise to FCs surrounding the most posterior egg chamber of newly-eclosed adults. These Fas3-positive cells, which we named Extra-Germarial Crown (EGC) cells in recognition of their location and appearance, accumulate from a handful to over twenty during the first 48h APF and then participate in an unprecedented set of dramatic morphological changes that produce the first egg chamber. During this process the most mature germline cyst leaves the germarium without accompanying ICs, enters EGC territory and moves a considerable distance from the germarium as it is enveloped by EGC cells. EGC cells were first defined in fixed images as expressing both TJ and Fas3 but live imaging showed that a few cells beyond the TJ-positive domain are also incorporated as FCs. Towards the end of the budding process cells posterior to the new egg chamber are intercalated to a width of two cells or less, forming a basal stalk, and a secondary EGC of Fas3-positive cells has accumulated between the germarium and the budded egg chamber. Secondary EGCs likely receive the second most mature cyst from the germarium but we have not observed that

budding process directly to know whether the budding cyst retains germarial ICs or principally recruits secondary EGCs as FCs, as suggested by lineage analyses. The budding of subsequent egg chambers likely mirrors the process in adults as there is no longer a recognizable EGC and the two most mature germline cysts are now surrounded by Fas3-positive cells within the germarium.

Our conclusions about the origin of adult FSCs and those regarding derivation of the first FCs from a newly-recognized EGC structure have some common ground and some differences relative to another recent study that used single cell RNA sequencing to explore the diversity of precursors in mature larvae and their adult fates. Of most relevance here, it was suggested that a distinct group of cells characterized by *bond-GAL4* expression, termed “FSCP”s for FSC and FC Progenitors, and located posterior to ICs, give rise to FSCs and FCs but not ECs (Slaidina et al., 2020). The principal supporting evidence is a cell lineage study with *bond-GAL4* induced cell marking intended to initiate during larval stages of development (by shifting from 29C to 18C shortly after pupariation). Lineages were found in 2d-old adults to include germarial FCs, implying that an FSC had been labeled in newly-eclosed adults (FSCs were not scored directly) but labeled ECs were also seen. The authors proposed that marked FSCs arose from FSCPs and marked ECs arose from labeling a different cell type, presumably an IC prior to pupariation (due to broader expression of *bond-GAL4* than *bond*). However, no clear evidence was presented that lineages had been initiated at the intended time or that ovarioles containing both marked FSCs and ECs contained two independent lineages; also, the frequency of ovarioles with marked FSCs (rather than FSCs or FCs) and no marked ECs was not reported because that can only be ascertained by scoring those cell types directly in newly-eclosed adults (Slaidina et al., 2020).

We repeated a *bond-GAL4* lineage analysis. We found that the time of initiation for clones containing ECs and FSCs was not controlled effectively by temperature shifts (in our hands) but was nevertheless likely to be prior to pupariation in most cases. We saw aggregate outcomes broadly similar to those previously reported, with frequent labeling of ECs, FSCs and FCs, though we saw a much higher fraction of ovarioles containing only labeled ECs. Among 36 ovarioles with marked FSCs, all but one also included marked ECs. Also, because we examined newly-eclosed adults we could cleanly distinguish and score all FSCs and FCs produced during development and we found that marked FSCs were always accompanied by marked FCs, while some ovarioles contained marked FCs but no marked FSCs. The labeled ovarioles contained considerably more marked ECs and FSCs than in our MARCM analyses. By making a simplifying assumption (a guessed approximation of reality) that each ovariole contained exactly two marked lineages, we calculated the frequency and content of different types of lineage originating from single cells. Both the proportions of different types of lineage and the average number of marked ECs and FSCs within each lineage corresponded quite closely to

the results obtained by inducing clones with *hs-flp* at pupariation. Those lineages, in both cases, included only ECs, ECs together with FSCs, but almost never FSCs without ECs. Thus, lineage analysis with *bond-GAL4* was not as informative as inducing lineages with *hs-flp* (using MARCM and multicolor marking) because it did not prove possible to define the time of lineage initiation through temperature manipulation or to study single cell lineages directly but the results were nevertheless fully in accord with our observations of lineages induced using *hs-flp*.

Our MARCM studies showed that the "decision" of a precursor to become an FSC rather than an EC plays out over a long period of time and that the majority of FSC-producing precursors have not segregated from EC-producing precursors until mid-pupation. Hence, the population of 14-16 adult FSCs cannot possibly derive largely or entirely from a distinctive cell type that is an FSC/FC-specific precursor at the end of larval development, as has been suggested (Slaidina et al., 2020). Equally important, pupal precursors that produce FSCs almost invariably also give rise to FCs of newly-eclosed adults, showing that there is no strict delineation of FSC precursor fates from either EC or FC fates at the start of pupation.

The expression pattern of the *bond* gene was described as spanning all ICs and then refining in late third instar larvae to the extreme margin of ICs and slightly posterior (Slaidina et al., 2020). Our live imaging studies suggest that cells in the latter locations are likely to contribute substantially to the EGC and then to FCs of the first budded egg chamber, a location where *bond-GAL4* activity was later detected in our study. Moreover, we found that *bond-GAL4* induced lineages that labeled only FCs in the terminal egg chamber of newly-eclosed adults if animals were raised at 29C (to elevate *bond-GAL4* activity and inactivate inhibitory GAL80 activity) for periods that included the first 2d or the last 3d of pupation. Although the window of thermosensitivity will need to be refined further, these results suggest that bond expression and bond-GAL4 activity may be selectively enriched in EGC cells and their products over a period preceding and following the budding of the first egg chamber at around 56h APF.

Extracellular signals that govern precursor movements and fate

We identified two signaling pathways that influence the AP location and consequent fate of precursors. The relevant tests all involved altering the genotype of a labeled lineage within the context of a large excess of normal precursors and therefore report consequences that are cell autonomous and reflect the behavior of labeled cells relative to normal neighbors. Reduction of Wnt signaling greatly reduced production of r1 ECs, suggesting that Wnt pathway activity must exceed a certain threshold for a cell to remain in the anterior third of the developing germarium. A Fz3-RFP reporter of Wnt pathway

activity is uniformly highest in this region throughout pupation, with the absolute magnitude increasing significantly over the first 36h APF. The production of FSCs was increased by elimination of Wnt pathway activity (using a null *arr* mutation) but was unaffected by just reducing pathway activity (by expression of dominant-negative TCF). These observations suggest that in more posterior regions where Wnt pathway activity normally declines roughly linearly towards zero, posterior movement from an EC-producing to an FSC-producing location is restrained by even low pathway activity. The influences of Wnt pathway magnitude during pupal development are very similar to those observed on AP location and EC/FSC choices in adult ovaries (Reilein et al., 2017).

JAK-STAT signaling also affects pupal ovary development but our investigations are less complete than for Wnt signaling because we have not conducted a detailed time-course of lineage analyses and because of the nature of the initial phenotypes we identified. We found that increasing JAK-STAT activity greatly increased the number of labeled cells per clone and in almost all cases greatly distorted germarial morphology, preventing us from classifying and counting marked cell types. Future tests will require a second genetic change to reduce precursor cell proliferation.

In normal developing ovaries we cannot clearly detect JAK-STAT activity at early stages. Reporter activity was seen only after the first egg chamber has budded and was seen in a posterior to anterior gradient that intensified over time, suggesting that, as in adults, polar cells may be a critical source of this graded JAK-STAT signaling pattern. Because pathway activity is initially low and remains low in anterior ICs genetic overexpression of STAT is likely to increase pathway activity very substantially over normal levels in anterior precursors and in all precursors over the first 48h APF, consistent with the large effects we observed on cell proliferation. JAK-STAT pathway manipulations in either direction produced large effects on cell proliferation in adult germarial cells (Vied et al., 2012).

Loss of JAK-STAT pathway activity from the beginning of pupation onwards resulted in a large cell autonomous reduction in the production of FSCs and FCs, with a corresponding increase in EC production, closely resembling the effects of excess Wnt pathway activity. The temporal focus of this effect has not been defined but it seems most likely to be in the latter stages of pupation because it is only during that time that we can detect significant levels of pathway activity using a stat-GFP reporter. Results from elevating Wnt pathway activity from -2d onwards show that two days can indeed suffice to reduce FSC production substantially in favor of ECs. Stat mutant precursors did not show any loss in cellular yields but very few of those cells and their descendants were likely in sufficiently posterior locations to be exposed to JAK-STAT ligand. We speculate that graded JAK-STAT pathway activity during the second half of pupation is important for stimulating proliferation of more posterior cells while anterior ICs slow and cease division.

Thus, our evidence to date suggests that graded Wnt signaling throughout pupation and graded JAK-STAT signaling during the second half of pupation are key organizers of the distribution of cells along the AP axis and their consequent final acquisition of EC and FSC fates. The relative proportions of adult ECs and FSCs produced are in part set by specifying a territory of precursors that give rise only to ECs and through the amplification of more posterior early precursors that produce both ECs and FSCs. These territories are influenced at the level of individual cells by the strength of Wnt pathway activity and a dependence on JAK-STAT signaling, suggesting that the evolving patterns of activity of these two pathways may be substantially responsible for dynamically defining EC, EC/FSC and FSC-producing domains. EC and FSC numbers also depend on the changing rates of precursor divisions in different locations. We speculate that JAK-STAT signaling has a key role in selectively promoting posterior cell proliferation after mid-pupation but we do not know which signals might regulate earlier proliferation, which also appears to be graded from anterior (low) to posterior.

It is likely that additional signaling pathways influence both the proliferation and location of precursors during pupal development. Delta signaling to Notch from terminal filament cells is important to specify adjacent cells as non-dividing Cap Cells roughly co-incident with the start of pupation (Gancz and Gilboa, 2013; Gancz et al., 2011; Panchal et al., 2017; Song et al., 2007; Yatsenko and Shcherbata, 2018). It was also previously shown that IC cells are distinguished from more posterior basal stalk cells prior to pupation through exposure to higher levels of Hh, emanating principally from terminal filament cells (Lai et al., 2017). It will be interesting to test whether Hh signaling affects the preference of a precursor to become an EGC or an IC, or EC, FSC and FC fates among ICs.

Coordination between germline and somatic ovarian cell development

Ovary development not only specifies suitable numbers of FSCs, GSCs and their niche cells but also prepares adults for producing mature eggs shortly after eclosion by producing a succession of maturing germline cysts in the germarium followed by four egg chambers. We have learned more about how pupal oogenesis is organized for both somatic and germline cells, providing a foundation for future exploration of coordination between the two.

It has been shown previously that germline differentiation is repressed globally prior to recruitment of anterior PGCs as future GSCs, at least in part through Ecdysone signaling acting on somatic cells (Gancz et al., 2011; Zhu and Xie, 2003). Then, late in third instar larvae, Ecdysone acts positively in somatic cells, via the Broad transcription factor, to initiate GSC differentiation, potentially in two steps of initial differentiation, evident from Bag-of-marbles (Bam) induction, and then cystocyte formation, revealed by the transition of the spectrosome to a fusome (Gancz and Gilboa, 2013; Gancz

et al., 2011). Those studies did not, however, reveal whether Bam-GFP expression or PGC division initiates simultaneously in all PGCs distant from Cap Cells or in an anterior-posterior gradient at the larval /pupal transition or how germline differentiation proceeds thereafter.

We found that there is a clear anterior to posterior polarity of increasingly developed cysts throughout pupal development. This was deduced by counting the number of germline cells linked by fusomes, with 16-cell cysts first appearing 18h APF, and by observing the exclusion of EdU DNA replication signals from the most posterior regions of the germarium from 36h onwards. Moreover, a single most posterior sixteen-cell cyst emerged for the first time between 36h and 48h APF. These observations raise a number of questions. First, what underlies the spatially organized initiation or progression of differentiation of PGCs that are in different locations at the larval/pupal transition? The Dpp signals that maintain anterior pre-GSCs are likely highly spatially restricted, as in adults, while hormonal Ecdysone signals are likely uniform, suggesting that there must be other important differentiation signals. Second, how is the posterior progression of increasingly mature cysts, starting from single anterior cells, organized?

The differentiation of germline cysts in the adult germarium depends on interactions with ECs and this has also been seen in some cases during pupal development even though many EC precursors are still dividing during early pupation. Normal Wnt pathway activity is among those shown to be important for this function in ECs and pre-ECs (Hamada-Kawaguchi et al., 2014; Luo et al., 2015; Mottier-Pavie et al., 2016; Upadhyay et al., 2018; Waghmare and Page-McCaw, 2018; Wang et al., 2015; Wang and Page-McCaw, 2018). It is not known what drives ordered posterior movement of germline cysts in adult germaria but this also may depend on EC interactions (Banisch et al., 2017). In future it will be interesting to investigate whether pupal or adult ECs have graded EC adhesive properties or send graded differentiation signals according to their AP position, instructed for example by the strength of Wnt signaling.

A second major focus for germline and somatic cell interactions is the budding of an egg chamber. The process necessarily involves a germline cyst leaving the germarium and establishing a lasting interaction with dividing FCs sufficient to envelop it in a monolayer epithelium. In an adult germarium a stage 2b cyst is enveloped by Fas3-positive FCs, which then proliferate and progress towards an epithelial morphology for another 12h before a rounded stage 3 cyst buds from the germarium. Remarkably, the order of events is reversed for the first egg chamber to bud from a pupal ovary, with a rounded germline cyst emerging from the germarium before being enveloped over a period of a few hours by extra-germarial Fas3-positive EGC cells. The common factor is that germline cysts in both cases progress through somatic cell territory (ECs and FSCs, or ICs) with low or absent

Fas3 expression and mesenchymal character but are captured by Fas3-positive cells that are developing an epithelial character.

The signals that guide development of Fas3-positive FCs have not been clearly defined but the location of those cells in the adult germarium suggests that low Wnt pathway activity and high JAK-STAT pathway activity may be important. Indeed, in both adult and pupal ovaries the onset of strong Fas3 expression coincides with the location where Wnt pathway activity drops to very low levels. Prior to budding of any egg chambers there is no polar FC source of JAK-STAT pathway ligand and we could not detect pathway activity in the germarium, potentially explaining the failure of ICs to acquire high levels of Fas3 expression and incipient FC qualities before 60h APF. Perhaps in this situation somatic cells must move even further from the range of anterior Wnt and potentially other signals (like Hh) to an EGC location in order to acquire those pre-FC characteristics in preparation for capturing a germline cyst that is pushed out of the germarium without an epithelial covering. Further comparative study of egg chamber formation in adult and pupal ovaries should help to resolve the key organizing principles behind cyst envelopment.

Acknowledgments

This work was supported by NIH RO1 GM079351 to DK. We thank Ruth Lehmann, Dorothea Godt, Erika Bach, Ramanuj DasGupta and Ward Odenwald for reagents, Pegah Kohosravi-Kamrani, Shay Mallick, Aaron Choi and Jack Misner for help with experiments and analysis, David Melamed for continued discussions and input, the Bloomington stock center for provision of genetic reagents, the Developmental Studies Hybridoma Bank (DSHB) for antibodies, FlyBase as an information resource, and the confocal microscope resource provided by the Dept. of Biological Sciences, Columbia University.

Conceptualization, A.R. and D.K., Formal Analysis, D.K., Funding Acquisition, D.K., Investigation, A.R., H.K., R.M. K.P., Methodology, H.K., K.P., A.R., R.M. D.K., Supervision, A.R. and D.K., Validation, A.R., H.K., R.M., K.P., D.K., Visualization, A.R., H.K., R.M., Writing-Original Draft, D.K., Writing-Review & Editing, A.R., H.K., R.M., K.P., D.K.

Methods

Staging of pupae

Third-instar larvae were sorted to select females, transferred to a vial with food and checked every hour to mark the time each individual developed into a puparium (white, but immobile, with small anterior spiracles). This time is 0 hours APF (after puparium formation). We found that keeping animals in the light at night and in the dark during the day on a 12h/12h cycle, allowed more of them to pupate during the daytime. We used a programmable outlet timer (Nearpow) together with a manual LED soft white nightlight (Energizer cat. 37099) installed in a dark incubator at 25C.

Dissection and staining of pupal ovaries.

Pupae were removed from the vial wall by adding a drop of water and transferred with forceps into a well of a Corning PYREX glass spot plate (Corning, cat. no. 7220–85) containing either PBS or 4% paraformaldehyde solution with care taken not to damage or pierce the posterior end of the pupa. If the dissection was done in fixative solution, it could take no longer than 10 min (ovaries were rocked in clean fixative for a minimum of 15 min, but for no longer than 30 min). Ovaries from 72h APF and older had fewer tears in them when dissected directly into fixative. Using a dissecting microscope, pupae were held against the bottom of the well using forceps and the posterior tip was cut off using Vannas Spring Scissors (2.5mm straight edge, Fine Science Tools, Foster City, CA, item number 15000-08) about a third of the way in from the posterior end. The anterior part of the pupa was removed to a discard well. The posterior end was searched for ovaries (clear, spherical, striated structures) by gently dislodging fat tissue surrounding the ovaries so as to not cloud the well with debris. This was done by gently tearing apart the contents of the pupal case or swirling them in the well using two pairs of forceps. As soon as they were spotted, ovaries were transferred to a new well of fixative by the following process. A 20µl pipette tip with a pipettor set to 20µl was coated in 10% Normal Goat Serum (NGS) by pipetting up and down several times. The pipettor was set to 5µl to pipette up the ovary from the dissection well to transfer into the fixative well. Ovaries were fixed by rocking ovaries in the well for 15 min at room temperature. Fixative was removed with a 1000µl pipette set to 270µl to slowly and carefully pipette up the liquid. The 1000 µl pipettor was used to remove liquid after all subsequent steps. Ovaries were rinsed 3x in 2% PBST 0.5% Tween solution for 5, 10, and 45 min at 4C by rocking very slowly in a horizontal plane. The glass dissection dish was covered with a large pipette tip box. Ovaries were rinsed for 30-60 min in 10% NGS solution at 4C, and then rocked gently in primary antibody overnight. Ovaries were rinsed 3x with 0.5% PBST and then incubated for 1 hour (covered, cold room, rocker set on 2) in secondary antibody diluted 1:1000 with 0.5% Triton. Rinse ovaries 2x

with 0.5% PBST and 1x with PBS. To mount ovaries, a 20µl pipette tip coated in 10% NGS solution as described above was set to 5µl and used to capture the ovary and transfer to a glass slide. 20µl of DAPI Fluoromount was added to a coverslip, and then placed on top of the slide with the ovaries. Care was taken to avoid pressing the coverslip and potentially disfiguring the mounted ovaries. For older pupal ovaries, specifically 72h APF and onwards, forceps were used to gently tear apart the ovarioles to separate germaria for clearer imaging. A sharpie was used to draw arrows to mark the location of the ovaries.

EdU labeling.

Ovaries were dissected directly into 15µM EdU in Schneider's insect medium, incubated for 1h at room temperature and then fixed for 10 min at room temperature in 4% paraformaldehyde. EdU incorporation was detected using the Click-iT Plus EdU Imaging Kit C10637 (Life Technologies).

Immunohistochemistry.

Monoclonal antibodies against LaminC, Fasciclin III, Vasa and Hts were obtained from the Developmental Studies Hybridoma Bank, created by the NICHD of the NIH and maintained at The University of Iowa, Department of Biology, Iowa City, Iowa 52242. 7G10 anti-Fasciclin III was deposited to the DSHB by C. Goodman, and was used at 1:300 for multicolor lineage experiments and at 1:250 in all other stainings. 1B1 anti-Hts was deposited by H.D. Lipshitz. LC28.26 Anti-LaminC at 1:50 was deposited by P.A. Fisher. Anti-Vasa (used at 1:10) was deposited by A. C. Spradling/D. Williams and used for staining adult ovaries. For pupal ovaries, the monoclonal rat anti-Vasa was not effective and instead rabbit anti-Vasa (gift from R. Lehmann, NYU medical school) was used. Other primary antibodies used were rabbit anti-Zfh-1 at 1:5000 (a gift from R. Lehmann, NYU medical school), guinea pig anti-Traffic Jam at 1:5000 (a gift from Dorothea Godt, University of Toronto, Canada), anti-β-galactosidase (Catalogue No. 55976, MP Biomedicals) at 1:1,000; anti-GFP (A6455, Molecular Probes) at 1:1,000; goat FITC-anti-GFP (Abcam ab6662) at 1:400. Secondary antibodies were Alexa-488, Alexa-546, Alexa-594 or Alexa-647 from Molecular Probes. Ovarioles from multicolor experiments were mounted in Prolong Gold Antifade (Invitrogen). DAPI-Fluoromount-G (Southern Biotech) was used as mounting medium for all other experiments. Images were collected with a Zeiss LSM700 or LSM800 laser scanning confocal microscope (Zeiss) using a 63x 1.4 N.A. lens.

Adult ovary fixation and staining.

Ovaries were fixed in 4% paraformaldehyde in PBS for 10 min at room temperature, rinsed three times in PBS with 0.1% Triton and 0.05% Tween-20 (PBST), and blocked in 10% normal goat serum

(Jackson ImmunoResearch Laboratories) in PBST. Ovarioles were incubated in primary antibody for 45 min for multicolor lineage experiments and overnight for all other experiments. Ovarioles were rinsed in PBST three times and incubated for 1 h in secondary antibodies diluted 1:1000.

Imaging and quantitation of Frizzled3-RFP.

Fz3-RFP flies (made by Ramanuj DasGupta, Genome Institute of Singapore and a gift from Erika Bach, NYU, USA) were dissected and stained for Fas3 and DAPI. Ovaries were imaged with a 63 × 1.4 N.A lens on a Zeiss LSM 800 confocal microscope (Carl Zeiss). Zeiss Zen Blue was used to acquire microscope images of 1024x1024 pixels at 16-bit depth with line averaging 2. Zeiss Zen was used to measure the intensity of RFP in cells along an edge of a germarium in a line from just next to Cap cells and ending at the border of Fas3 expression. Measurements were taken in 5 μm distance increments within a z-stack range that did not exceed 8 μm. If there were more than one cell within the same 5 μm increment, both cells would be measured. If there were no suitable cell within the 8 um z-stack range at a specific 5 um increment, no measurement was collected. Fz3-RFP intensities were measured by circling the nucleus of a cell in the DAPI channel using the spline contour tool and obtaining the average intensity value in the 561 channel for the enclosed area from the Z-stack with the highest RFP intensity. The 561 laser intensity was set at 1.1% for 21-36h APF germaria and reduced to 0.3% beginning at 48h-APF through adult in order to keep RFP within the linear range. Because germaria in early z-slices were brighter than germaria in later z slices, RFP intensities for each germarium were normalized to the brightest cell on the edge of that gemarium. Normalized intensities were then averaged for each time point. In order to reflect the relative RFP brightness from 27h to 36h-APF, the averaged, normalized values were divided by the laser intensity at which they were taken. The averaged normalized values for every distance along the 27h-APF and 36-APF curves were divided by 1.1. The averaged normalized values for every distance along the 48h-APF, 60h-APF, and Adult curves were divided by 0.3. The 27h-APF, 36h-APF, 48h-APF, 60h-APF, and adult were then normalized to the highest value in all of the graphs to reflect relative intensities while preserving the Wnt gradient shape. In order to depict the relative RFP brightness for the 21h and 27h-APF germaria in the figure, output levels from 255 to 100 in Photoshop. The distances from Cap cells to the border of strong Fas3 expression on the edge of the germarium and to the posterior end of the germline in the center of the germarium were also measured for every germarium and averaged for each time-point.

Live imaging and analysis.

Live imaging was performed as in (Reilein et al., 2018a). Imaged ovaries were of genotype *yw hs-flp; ubi-GFP FRT40A* or *yw hs-flp/yw; ubi-GFP FRT40A FRT42B His2Av-RFP/tub-lacZ FRT40A FRT42B*.

Images were acquired every 15 min with 2.5 µm between Z-stacks. Clones were generated in the GFP/RFP ovaries by two 10 min heat shocks at 37° spaced 8 hours apart, 48 to 72 hours before imaging in order to generate GFP-only and RFP-only cells that were easier to track. Volocity Software (Quorum Technologies, Puslinch, Ontario, Canada) was used to make the 4D reconstruction of the UbiGFP labeled ovary. All nineteen z slices covering 45 µm were used in the reconstruction; however germaria drifted during imaging such that FCs covering approximately one quarter of the budded egg chamber on the lower germarium were not imaged. Cells were colored with Procreate software (Savage Interactive, North Hobart, Australia). Germline cells in the UbiGFP movie were identified based on their larger size and paler labeling with GFP compared to somatic cells.

Markers and clonal analysis of mutant genotypes.

Flies with alleles on an *FRT42D* or *FRT82B* chromosome were used in MARCM experiments:
FRT42D: *hs-Flp, UAS-nGFP, tub-GAL4; FRT42D act-GAL80 tub-GAL80 / FRT42D (X); act>CD2>GAL4/* + where X was *ubi-GFP* (Control) or arr^{2} (> indicates an *FRT* site)
FRT82B: *hs-Flp, UAS-nGFP, tub-GAL4; act>CD2>GAL4 UAS-GFP / +; FRT82B tub-GAL80/FRT82B (X)* – where X was *NM* (control), $stat^{06346}$, axn^{E77}, $apc1^{Q8}apc2^{D40}$, $UAS\text{-}Hop^{3W}$ *or UAS-dnTCF*
For multicolor clones flies were of the genotype: *yw hs-flp; ubi-GFP FRT40A* or *yw hs-flp/yw; ubi-GFP FRT40A FRT42B His2Av-RFP/tub-lacZ FRT40A FRT42B*
Genotypes for FLY-FUCCI were *C587-GAL4/ yw; UAS-FUCCI/Cyo; UAS-FUCCI/ (UAS-FUCCI or TM6B)*.
Two copies of *stat-GFP* were required to obtain a GFP signal in pupal ovaries (one is sufficient in adults).

Lineage analysis by MARCM

Pupae were heat shocked at 33C for 12 min at the number of days indicated before eclosion. Flies were dissected on the day of eclosion (0d MARCM) or collected on the day of eclosion and dissected 2 days later. Ovaries were stained for Vasa, Fas3 and GFP. Cells were scored as r1 or r2a based on measurements that were performed to determine the lengths of these regions. To determine the boundaries of each region we examined EdU incorporation in ovaries of newly eclosed flies and measured the distance from cap cells to the end of Region 1 as determined by the presence of cysts that incorporated EdU. Region 1 cysts are going through mitosis and Region 2a cysts have the

complete complement of 16 germ cells. The length ratio of Region 1:2a is about 3:1 in newly-eclosed adults.

bondGal4/G trace experiments

bond-GAL4/G-TRACE flies (a gift of Ruth Lehmann, NYU medical center) were crossed at 18C and either kept at 18C, shifted after egg-laying to 29C and shifted back to 18C in mid-pupation (flies took 6 more days to eclose at 18C); or shifted to 29C 3 to 4 days before eclosion. Flies were dissected on the day of eclosion.

Inferring clone types, FSC and EC numbers in newly-eclosed adults from scoring 2d-old adults

In order to make quantitative conclusions about the developmental process up to eclosion from scoring clonal outcomes in 2d-old adults we made the following assumptions and adjustments. We assumed that EC numbers and locations did not change during this 2d interval because ECs generally appear to be quite long-lived. ECs are, however, produced from FSCs during adulthood, so it is likely that a small number of marked ECs scored at +2d were produced from FSCs after eclosion. The proportion of marked ECs arising from FSCs is very likely small based on known rates of FSC conversion to ECs and the observed high frequency of FSC clones with no ECs (44%) from -2d samples. Individual marked FSCs can be lost, mainly by becoming FCs, or amplified at high rates during adulthood. If one or more marked FSCs were present at 0d but became FCs by +2d those marked FCs would reside around the two germarial cysts or in the two youngest egg chambers because egg chambers bud roughly every 12h, allowing four cycles of FC recruitment over 2d. We therefore scored an ovariole as containing an FSC clone (FSC-only or FSC/EC, according to EC content) if there were any marked FCs up to and including the second egg chamber, even if there were no FSCs at +2d. In those cases we scored the number of marked FSCs as zero. On average, the number of marked FSCs should remain constant from 0d to +2d, so we should obtain a very good estimation of FSC numbers at 0d by scoring the numbers of marked FSCs at +2d, provided we include all examples where marked FSCs were lost altogether as containing zero FSCs. By using these guidelines we could surmise the exact number of different types of clone at 0d and the exact number of constituent ECs and FSCs from data collected by scoring clones in 2d-old adults.

Calculation of single-cell lineage frequencies correcting for ovarioles containing more than one lineage

A. Assuming independent recombination events

The proportion of marked ovarioles with a lineage originating from a single marked cell was first estimated by assuming that the probability of each dividing precursor to be labeled was independent. The estimate derives principally from the observed frequency of labeled ovarioles but it is also dependent (to a lesser extent) on the number of potential target cells. Different numbers of assumed target cells are used in the calculations below to demonstrate that estimated single cell frequencies are not greatly altered by this value.

For the -6d to -2d time course, the average frequency of labeled ovarioles was about 60%. If there were only 6 target cells (estimated for -6d), assuming a binomial distribution (independent probabilities), the chance of any one cell giving a clone is p and the chance of 6 cells not giving a clone is $(1-p)^6$. The observed no-clone fraction was 0.4, so (1-p)= 0.86 and p =0.14. Hence, the single clone frequency among 6 cells is $6p(1-p)^5$, and the frequency among labeled ovarioles is 1/0.6 fold higher (because 60% were labeled). Therefore, the expected frequency of single-cell lineages is $6x0.14x(0.86)^5/0.6$= 0.66. If there were 15 target cells (estimated for -2d) then p = 0.06 (because 0.94^{15}= 0.4) and the frequency of single-cell lineages is $15x0.06x(0.94)^{14}/0.6$= 0.63. If there were 30 target cells then p = 0.03 (because 0.97^{30}= 0.4) and the frequency of single-cell lineages is $30x0.03x(0.97)^{29}/0.6$= 0.62.

For the multicolor experiment examining newly-eclosed adults 5d after heat-shock, the frequency of labeled ovarioles was 26/115 = 23%. If there were 20 target cells, then p = 0.013 (because 0.987^{20}= 0.77) and the frequency of single-cell lineages is $20x0.013x(0.987)^{19}/0.23$ = 0.86.

For the MARCM experiment examining newly-eclosed adults 5d after heat-shock, the frequency of labeled ovarioles was 33%. If there were 20 target cells, then p = 0.02 (because 0.98^{20}= 0.67) and the frequency of single-cell lineages is $20x0.02x(0.98)^{19}/0.33$ = 0.80.

B. Assuming lower frequencies of single lineages based on the frequency of ovarioles with marked ECs and FCs

In MARCM and multicolor lineage experiments scored in newly-eclosed adults we observed a higher than expected frequency of ovarioles with labeled ECs and FCs but no FSCs, which we assume represent two distinct lineages because the marked cells are discontinuous. The observation indicated that single cell lineages frequencies were lower than calculated (above) assuming independent

probabilities of precursor marking. Based on the EC/FC clone frequency and the proportion of unlabeled ovarioles we estimated that a specific proportion of labeled ovarioles harbored a single lineage, while the rest contained exactly two lineages. We settled on values that were roughly consistent with the observed frequency of ovarioles with marked ECs and FCs.

B1 MARCM clones induced 5d before eclosion

For the MARCM experiment examining newly-eclosed adults 5d after heat-shock, 67% of ovarioles were unlabeled. Single cell lineage frequencies and labeled cell content were calculated, as described below, assuming that 30% of ovarioles with marked cells derived from a single marked cell, while the remaining 70% derived from two marked cells. In all cases, EC/FSC and FSC-only categories include clones with and without FCs (aggregated).

pEC, pEC/FSC, pFSC, pFC are the proportions of each type of single-cell lineage amongst all marked lineages. Observed values are the proportion of marked ovarioles with the specific type(s) of cell. EC-only means no FSC. FC-only means no FSC. Both categories include EC+FC ovarioles.

Observed EC-only = 0.47 + 0.16 = 0.63 = 0.3 pEC + 0.7 $(pEC)^2$ + 1.4pEC.pFC

Observed FC-only = 0.09 + 0.16 = 0.25 = 0.3 pFC + 0.7 $(pFC)^2$ + 1.4pEC.pFC

Above satisfied by pEC= 0.63 and pFC= 0.19

Observed FSC-only = 0.03 = 0.3pFSC + 0.7 [$(pFSC)^2$ + 2pFSC.pFC]

= 0.7[$(pFSC)^2$ + 0.566pFSC

So, pFSC = 0.050

Hence, pEC/FSC = 1 – (pEC + pFSC + pFC)= 0.13

Observed ECs per EC-only ovariole = (2.4 x0.47 + 2.9 x 0.16)/ 0.63 = 2.53

Of double-clones in EC-only, 0.397/0.636= 0.624 are two EC clones and 0.239/0.636 = 0.376 are one EC and one FC clone

So, number of EC lineages per EC-only ovariole = 0.3 + 0.7(1.248 + 0.376) = 1.44

So ECs per EC-only lineage = 2.53/1.44 =1.76

Observed FSCs per FSC-only ovariole = 14/3

Of double-clones in FSC-only, 0.0025/0.215= 0.116 are two FSC clones and 0.019/0.215 = 0.884 are one FSC and one FC clone

So, number of FSC lineages per FSC-only ovariole = 0.3 + 0.7(0.232 + 0.884) = 1.08

So FSCs per FSC-only lineage = 14/(3x1.08) = 4.32

Total ovarioles with marked cells= 98, so total number of lineages= 98 x 1.7 = 166.6

Total ECs from EC-only lineages = 166.6pEC(1.76) = 184.7

Total FSCs from FSC-only lineages = 166.6pFSC(4.32) = 35.9

Total ECs scored = 253, total FSCs scored = 111

So, total ECs from EC/FSC clones = 68.3

Total FSCs from EC/FSC clones = 75.1

Total EC/FSC lineages = 166.6pEC/FSC = 21.66

So ECs per EC/FSC clone = 3.15, and FSCs per EC/FSC clone = 3.47

Deduced 24.0 precursors (to produce 16 FSCs): 15.1 pECs, 3.1 pEC/FSCs, 1.2 pFSCs, 4.6 pFCs.

B2 Multicolor clones induced 5d before eclosion

Analogous calculations for multicolor GFP-only clones where EC plus FC category was 8% and assuming 70% of marked ovarioles have lineages derived from one cell, and 30% have two lineages.

Observed EC-only = 0.423 + 0.077 = 0.50 = 0.7 pEC + 0.3 $(pEC)^2$ + 0.6pEC.pFC

Observed FC-only = 0.077 + 0.077 = 0.154 = 0.7 pFC + 0.3 $(pFC)^2$ + 0.6pEC.pFC

Above satisfied by pEC= 0.52 and pFC= 0.14

Observed FSC-only = 0.077 = 0.7pFSC + 0.3 [$(pFSC)^2$ + 2pFSC.pFC]

= 0.3[$(pFSC)^2$ + 0.778pFSC

So, pFSC = 0.095

Hence, pEC/FSC = 1 – (pEC + pFSC + pFC)= 0.245

Observed ECs per EC-only ovariole = 38/13 = 2.92

Of double-clones in EC-only, 0.2704/0.416 = 0.65 are two EC clones and 0.1456/0.416 = 0.35 are one EC and one FC clone

So, number of EC lineages per EC-only ovariole = 0.7 + 0.3(1.3 + 0.35) = 1.195

So ECs per EC-only lineage = 2.92/1.195 = 2.44

Observed FSCs per FSC-only ovariole = 4.0

Of double-clones in FSC-only, 0.00593/0.02363= 0.25 are two FSC clones and 0.0177/0.02363= 0.75 are one FSC and one FC clone

So, number of lineages per FSC-only ovariole = 0.7 + 0.3(0.50 + 0.75) = 1.0375

So FSCs per FSC-only lineage = 4.0/1.0375 = 3.86

Total ovarioles with marked cells= 26, so total number of lineages= 26 x 1.3 = 33.8

Total ECs from EC-only lineages = 33.8pEC(2.44) = 42.89

Total FSCs from FSC-only lineages = 33.8pFSC(3.86) = 10.04

Total ECs scored = 66, total FSCs scored = 29

So, total ECs from EC/FSC clones = 17.11

Total FSCs from EC/FSC clones = 18.96

Total EC/FSC lineages = 33.8pEC/FSC = 8.28

So ECs per EC/FSC clone = 2.07, and FSCs per EC/FSC clone = 2.27

Deduced 17.3 precursors (to produce 16 FSCs): 9.0pECs, 4.2 pEC/FSCs, 1.6 pFSCs, 2.0 pFCs.

B3. MARCM clones induced 3.5d before eclosion

Analogous calculations for MARCM clones induced at -3.5d, where EC plus FC category was 8% and assuming 70% of marked ovarioles have lineages derived from one cell, and 30% have two lineages.

Observed EC-only = 0.207 + 0.438 = 0.645 = $(pEC)^2$ + 2pEC.pFC

Observed FC-only = 0.091 + 0.438 = 0.529 = $(pFC)^2$ + 2pEC.pFC

Above satisfied by pEC= 0.51 and pFC= 0.38

Observed FSC-only = 0.033 = $(pFSC)^2$ + 2pFSC.pFC = $(pFSC)^2$ + 0.76pFSC

So, pFSC = 0.041

Hence, pEC/FSC = 1 – (pEC + pFSC + pFC)= 0.07

Of double-clones in FC-only, 0.144/0.532= 0.27 are two FC clones and 0.388/0.532 = 0.73 are one EC and one FC clone

Observed ECs per EC-only ovariole = 199/78 = 2.55

Of double-clones in EC-only, 0.260/0.646= 0.40 are two EC clones and 0.388/0.646 = 0.60 are one EC and one FC clone

So, number of EC lineages per EC-only ovariole = 0.8 + 0.6 = 1.40

So ECs per EC-only lineage = 2.55/1.40 =1.82

Observed FSCs per FSC-only ovariole = 13/4 = 3.25

Of double-clones in FSC-only, 0.00168/0.03284= 0.05 are two FSC clones and 0.03116/0.03284= 0.95 are one FSC and one FC clone

So, number of FSC-only lineages per FSC-only ovariole = 1.05

So FSCs per FSC-only lineage = 3.25/1.05 = 3.10

Total ovarioles with marked cells= 121, so total number of lineages= 242

Total ECs from EC-only lineages = 242pEC(1.82) = 224.6
Total FSCs from FC-only lineages = 242pFSC(3.10) = 30.8
Total ECs scored = 276, total FSCs scored = 111
So, total ECs from EC/FSC clones = 51.4
Total FSCs from EC/FSC clones = 80.2
Total EC/FSC lineages = 242pEC/FSC = 16.94
So ECs per EC/FSC clone = 3.03, and FSCs per EC/FSC clone = 4.73

Deduced 34.9 precursors (to produce 16 FSCs): 17.8pECs, 2.4 pEC/FSCs, 1.4 pFSCs, 13.3 pFCs. Also, by this time there are EC precursors that no longer divide (estimated at 5 for -4d and 18 for -3d from MARCM lineages examined in +2d adults, so perhaps 11.5 at -3.5d, to give a total of 45.4 precursors. So, estimated proportion of precursors that are pFCs is 13.3/45.4 = 29%.

B4 bond-GAL4/G-trace lineages

Single lineage frequencies and content for clones initiated by bond-GAL4were calculated in a slightly different way (considering ovarioles with only marked ECs to calculate EC-only single lineage and then ovarioles with labeled ECs and FCs clones to calculate the FC-only lineage frequency) because there were almost no ovarioles with only marked FCs.
Here we assumed that every labeled ovariole had exactly two lineages.
Observed EC frequency = 38.36% = $(pEC)^2$
So, pEC= 61.9%
Observed EC+FC frequency= 9.59% = 2pEC.pFC
So pFC = 7.75%
Observed FSC frequency = 1.37% = $(pFC)^2$ + 2pFC. pFSC
So, pFSC= 6.29%
Therefore pEC/FSC = 24.0%
Observed EC per EC-only (or EC+FC) lineage= 207/35= 5.91
Of double-clones in EC-only, expected frequencies: 0.383/0.479= 0.80 are two EC clones and 0.096/0.479 = 0.20 are one EC and one FC clone
So, number of EC lineages per EC-only ovariole = 2x 0.8 + 0.2= 1.8
So ECs per EC-only lineage = 5.91/1.8 =3.28
Ovariole with labeled FSCs but no ECs has 7 FSCs

Of double-clones in FSC-only, 0.00396/0.01371= 0.289 are two FSC clones and 0.00975/0.01371 = 0.721 are one FSC and one FC clone

So, number of FSC lineages per FSC-only ovariole = 2x0.289 + 0.721 = 1.32

So FSCs per FSC-only lineage = 7/1.32 = 5.3

Total ovarioles with marked cells= 73, so total number of lineages= 146

Total ECs from EC-only lineages = 146pEC(3.28) = 296.4

Total FSCs from FSC-only lineages = 146pFSC(5.3) = 48.7

Total ECs scored = 496, total FSCs scored = 190

So, total ECs from EC/FSC clones = 199.6

Total FSCs from EC/FSC clones = 141.3

Total EC/FSC lineages = 146pEC/FSC = 35.4

So ECs per EC/FSC clone = 5.64, and FSCs per EC/FSC clone = 3.99

Heat-shock to eclosion (days)	pr1		pr1/2a			pEC/FSC				pFSC	
	Freq.	Yield	Freq.	Yield		Freq.	Yield			Freq.	Yield
	%	r1	%	r1	r2a	%	r1	r2a	FSC	%	FSC
2	7.9	1.2	6.3	0.3	1.8	41	0.5	1.2	1.3	44	1.2
3	14	1.2	16	0.8	2.2	40	0.9	1	2.6	30	1.4
4	34	2.1	23	2	1.6	38	1.6	1.5	3.7	4.6	3
5	33	2.2	25	2.8	2.3	40	3.1	3.4	5.5	2.7	2.5
6	31	3.5	14	3.3	3.6	53	3.2	3.4	4.8	2.7	3

Table 1. Frequency of clones originating from different precursors and yields per clone.

Heat-shock to eclosion (days)	Total Number of marked cells in clones				Cells made per germarium from dividing precursors			
	r1	r2a	EC	FSC	r1	r2a	EC	FSC
	x	y	x+y	z	16x/z	16y/z	16(x+y)/z	
2	20	37	57	69	4.6	8.6	13.2	16
3	41	46	87	93	7.1	7.9	15	16
4	156	80	236	134	18.6	9.6	28.2	16
5	191	140	331	164	18.6	13.7	32.3	16
6	356	253	609	295	19.3	13.7	33	16

Table 2. Number of adult cells of each type made from dividing precursors at different developmental times calculated from the total yield of marked cells of each type.

	n	EC		EC/FSC			FSC		FC	EC+FC		Number of dividing precursors per germarium				
		Freq.	Yield	Freq.	Yield		Freq.	Yield	Freq.	Freq.	Yield	Total (n)	pEC	pEC/FSC	pFSC	pFC
		%	EC	%	EC	FSC	%	FSC	%	%	EC					
		100p		100q		x	100r	y	100s			16/ (qx+ry)	pn	qn	rn	sn
5-MARCM raw data	98	46.9	2.4	25	4	4	3	4.3	9.2	16.3	2.9					
5-MARCM assuming 70% double clones		63	1.8	13	3.2	3.5	5	4.3	19			24	15.1	3.1	1.2	4.6
5-Mulicolor raw data	26	42.3	3	31	3.5	2.6	7.7	4	12	7.7	2.5					
5-Multicolor assuming 30% double clones		52	2.4	25	2.1	2.3	9.5	3.9	14			17.3	9	4.2	1.6	2.4
3.5-MARCM raw data	121	20.7	2.5	23	2.8	3.5	3.3	3.3	9.1	43.8	2.6					
3,5-MARCM assuming all double clones		51	1.8	7	3	4.7	4.1	3.1	38			34.9	17.8	2.4	1.4	13
bond-GAL4 raw data	73	38.4	5.1	48	8.3	5.4	1.4	7	2.7	9.6	9					
bond-GAL4 assuming all double clones		61.9	3.3	24	5.6	4	6.3	5.3	7.8			15.1	9.4	3.6	1	1.2

Table 3. Clone frequencies and cellular yields from different lineage experiments together with deduced single-lineage parameters including the number of precursors of different types.

References

Asaoka, M., and Lin, H. (2004). Germline stem cells in the Drosophila ovary descend from pole cells in the anterior region of the embryonic gonad. Development *131*, 5079-5089.

Bach, E.A., Ekas, L.A., Ayala-Camargo, A., Flaherty, M.S., Lee, H., Perrimon, N., and Baeg, G.H. (2007). GFP reporters detect the activation of the Drosophila JAK/STAT pathway in vivo. Gene Expr Patterns *7*, 323-331.

Banisch, T.U., Maimon, I., Dadosh, T., and Gilboa, L. (2017). Escort cells generate a dynamic compartment for germline stem cell differentiation via combined Stat and Erk signalling. Development *144*, 1937-1947.

Cohen, E.D., Mariol, M.C., Wallace, R.M., Weyers, J., Kamberov, Y.G., Pradel, J., and Wilder, E.L. (2002). DWnt4 regulates cell movement and focal adhesion kinase during Drosophila ovarian morphogenesis. Dev Cell *2*, 437-448.

Dai, W., Peterson, A., Kenney, T., Burrous, H., and Montell, D.J. (2017). Quantitative microscopy of the Drosophila ovary shows multiple niche signals specify progenitor cell fate. Nature communications *8*, 1244.

Duhart, J.C., Parsons, T.T., and Raftery, L.A. (2017). The repertoire of epithelial morphogenesis on display: Progressive elaboration of Drosophila egg structure. Mech Dev *148*, 18-39.

Evans, C.J., Olson, J.M., Ngo, K.T., Kim, E., Lee, N.E., Kuoy, E., Patananan, A.N., Sitz, D., Tran, P., Do, M.T.*, et al.* (2009). G-TRACE: rapid Gal4-based cell lineage analysis in Drosophila. Nature methods *6*, 603-605.

Forbes, A.J., Spradling, A.C., Ingham, P.W., and Lin, H. (1996). The role of segment polarity genes during early oogenesis in Drosophila. Development *122*, 3283-3294.

Gancz, D., and Gilboa, L. (2013). Insulin and Target of rapamycin signaling orchestrate the development of ovarian niche-stem cell units in Drosophila. Development *140*, 4145-4154.

Gancz, D., Lengil, T., and Gilboa, L. (2011). Coordinated regulation of niche and stem cell precursors by hormonal signaling. PLoS biology *9*, e1001202.

Gehart, H., and Clevers, H. (2019). Tales from the crypt: new insights into intestinal stem cells. Nat Rev Gastroenterol Hepatol *16*, 19-34.

Gilboa, L. (2015). Organizing stem cell units in the Drosophila ovary. Curr Opin Genet Dev *32*, 31-36.

Godt, D., and Laski, F.A. (1995). Mechanisms of cell rearrangement and cell recruitment in Drosophila ovary morphogenesis and the requirement of bric a brac. Development *121*, 173-187.

Golic, K.G., and Lindquist, S. (1989). The FLP recombinase of yeast catalyzes site-specific recombination in the Drosophila genome. Cell *59*, 499-509.

Hamada-Kawaguchi, N., Nore, B.F., Kuwada, Y., Smith, C.I., and Yamamoto, D. (2014). Btk29A promotes Wnt4 signaling in the niche to terminate germ cell proliferation in Drosophila. Science *343*, 294-297.

Hayashi, Y., Yoshinari, Y., Kobayashi, S., and Niwa, R. (2020). The regulation of Drosophila ovarian stem cell niches by signaling crosstalk. Curr Opin Insect Sci *37*, 23-29.

Irizarry, J., and Stathopoulos, A. (2015). FGF signaling supports Drosophila fertility by regulating development of ovarian muscle tissues. Developmental biology *404*, 1-13.

Jemc, J.C. (2011). Somatic gonadal cells: the supporting cast for the germline. Genesis *49*, 753-775.

Kahney, E.W., Snedeker, J.C., and Chen, X. (2019). Regulation of Drosophila germline stem cells. Curr Opin Cell Biol *60*, 27-35.

King, R.C., Aggarwal, S.K., and Aggarwal, U. (1968). The development of the female Drosophila reproductive system. J Morphol *124*, 143-166.

Kirilly, D., Wang, S., and Xie, T. (2011). Self-maintained escort cells form a germline stem cell differentiation niche. Development *138*, 5087-5097.

Lai, C.M., Lin, K.Y., Kao, S.H., Chen, Y.N., Huang, F., and Hsu, H.J. (2017). Hedgehog signaling establishes precursors for germline stem cell niches by regulating cell adhesion. J Cell Biol *216*, 1439-1453.

Lee, T., and Luo, L. (2001). Mosaic analysis with a repressible cell marker (MARCM) for Drosophila neural development.[erratum appears in Trends Neurosci 2001 Jul;24(7):385]. Trends in Neurosciences *24*, 251-254.

Li, M., Hu, X., Zhang, S., Ho, M.S., Wu, G., and Zhang, L. (2019). Traffic jam regulates the function of the ovarian germline stem cell progeny differentiation niche during pre-adult stage in Drosophila. Sci Rep *9*, 10124.

Li, M.A., Alls, J.D., Avancini, R.M., Koo, K., and Godt, D. (2003). The large Maf factor Traffic Jam controls gonad morphogenesis in Drosophila. Nat Cell Biol *5*, 994-1000.

Luo, L., Wang, H., Fan, C., Liu, S., and Cai, Y. (2015). Wnt ligands regulate Tkv expression to constrain Dpp activity in the Drosophila ovarian stem cell niche. J Cell Biol *209*, 595-608.

Luo, X., Puig, O., Hyun, J., Bohmann, D., and Jasper, H. (2007). Foxo and Fos regulate the decision between cell death and survival in response to UV irradiation. Embo J *26*, 380-390.

Margolis, J., and Spradling, A. (1995). Identification and behavior of epithelial stem cells in the Drosophila ovary. Development *121*, 3797-3807.

Mottier-Pavie, V.I., Palacios, V., Eliazer, S., Scoggin, S., and Buszczak, M. (2016). The Wnt pathway limits BMP signaling outside of the germline stem cell niche in Drosophila ovaries. Developmental biology.

Murray, S.M., Yang, S.Y., and Van Doren, M. (2010). Germ cell sex determination: a collaboration between soma and germline. Curr Opin Cell Biol *22*, 722-729.

Panchal, T., Chen, X., Alchits, E., Oh, Y., Poon, J., Kouptsova, J., Laski, F.A., and Godt, D. (2017). Specification and spatial arrangement of cells in the germline stem cell niche of the Drosophila ovary depend on the Maf transcription factor Traffic jam. PLoS Genet *13*, e1006790.

Park, K.S., Godt, D., and Kalderon, D. (2018). Dissection and Staining of Drosophila Pupal Ovaries. Journal of visualized experiments : JoVE.

Reilein, A., Cimetta, E., Tandon, N.M., Kalderon, D., and Vunjak-Novakovic, G. (2018a). Live imaging of stem cells in the germarium of the Drosophila ovary using a reusable gas-permeable imaging chamber. Nature protocols *13*, 2601-2614.

Reilein, A., Melamed, D., Park, K.S., Berg, A., Cimetta, E., Tandon, N., Vunjak-Novakovic, G., Finkelstein, S., and Kalderon, D. (2017). Alternative direct stem cell derivatives defined by stem cell location and graded Wnt signalling. Nat Cell Biol *19*, 433-444.

Reilein, A., Melamed, D., Tavare, S., and Kalderon, D. (2018b). Division-independent differentiation mandates proliferative competition among stem cells. Proc Natl Acad Sci U S A *115*, E3182-E3191.

Sahai-Hernandez, P., and Nystul, T.G. (2013). A dynamic population of stromal cells contributes to the follicle stem cell niche in the Drosophila ovary. Development *140*, 4490-4498.

Sahut-Barnola, I., Dastugue, B., and Couderc, J.L. (1996). Terminal filament cell organization in the larval ovary of Drosophila melanogaster: ultrastructural observations and pattern of divisions. Roux Arch Dev Biol *205*, 356-363.

Slaidina, M., Banisch, T.U., Gupta, S., and Lehmann, R. (2020). A single-cell atlas of the developing Drosophila ovary identifies follicle stem cell progenitors. Genes Dev *34*, 239-249.

Song, X., Call, G.B., Kirilly, D., and Xie, T. (2007). Notch signaling controls germline stem cell niche formation in the Drosophila ovary. Development *134*, 1071-1080.

Tworoger, M., Larkin, M.K., Bryant, Z., and Ruohola-Baker, H. (1999). Mosaic analysis in the drosophila ovary reveals a common hedgehog-inducible precursor stage for stalk and polar cells. Genetics *151*, 739-748.

Upadhyay, M., Kuna, M., Tudor, S., Martino Cortez, Y., and Rangan, P. (2018). A switch in the mode of Wnt signaling orchestrates the formation of germline stem cell differentiation niche in Drosophila. PLoS Genet *14*, e1007154.

Valer, F.B., Machado, M.C.R., Silva-Junior, R.M.P., and Ramos, R.G.P. (2018). Expression of Hbs, Kirre, and Rst during Drosophila ovarian development. Genesis *56*, e23242.

van de Wetering, M., Sancho, E., Verweij, C., de Lau, W., Oving, I., Hurlstone, A., van der Horn, K., Batlle, E., Coudreuse, D., Haramis, A.P.*, et al.* (2002). The beta-catenin/TCF-4 complex imposes a crypt progenitor phenotype on colorectal cancer cells. Cell *111*, 241-250.

Vied, C., and Kalderon, D. (2009). Hedgehog-stimulated stem cells depend on non-canonical activity of the Notch co-activator Mastermind. Development *136*, 2177-2186.

Vied, C., Reilein, A., Field, N.S., and Kalderon, D. (2012). Regulation of stem cells by intersecting gradients of long-range niche signals. Dev Cell *23*, 836-848.

Vlachos, S., Jangam, S., Conder, R., Chou, M., Nystul, T., and Harden, N. (2015). A Pak-regulated cell intercalation event leading to a novel radial cell polarity is involved in positioning of the follicle stem cell niche in the Drosophila ovary. Development *142*, 82-91.

Waghmare, I., and Page-McCaw, A. (2018). Wnt Signaling in Stem Cell Maintenance and Differentiation in the Drosophila Germarium. Genes (Basel) *9*.

Wang, S., Gao, Y., Song, X., Ma, X., Zhu, X., Mao, Y., Yang, Z., Ni, J., Li, H., Malanowski, K.E.*, et al.* (2015). Wnt signaling-mediated redox regulation maintains the germ line stem cell differentiation niche. Elife *4*, e08174.

Wang, X., and Page-McCaw, A. (2014). A matrix metalloproteinase mediates long-distance attenuation of stem cell proliferation. J Cell Biol *206*, 923-936.

Wang, X., and Page-McCaw, A. (2018). Wnt6 maintains anterior escort cells as an integral component of the germline stem cell niche. Development *145*.

Yatsenko, A.S., and Shcherbata, H.R. (2018). Stereotypical architecture of the stem cell niche is spatiotemporally established by miR-125-dependent coordination of Notch and steroid signaling. Development *145*.

Zhu, C.H., and Xie, T. (2003). Clonal expansion of ovarian germline stem cells during niche formation in Drosophila. Development *130*, 2579-2588.

Zielke, N., Korzelius, J., van Straaten, M., Bender, K., Schuhknecht, G.F., Dutta, D., Xiang, J., and Edgar, B.A. (2014). Fly-FUCCI: A versatile tool for studying cell proliferation in complex tissues. Cell Rep *7*, 588-598.

Figure Legends

Figure 1. Development of adult germaria during early pupal stages.

(A-J) A time-course of pupal ovary development with **(J)** cartoons highlighting individual germaria from 12h APF, 30h APF and adults. Vasa (green) marks germline cells, Traffic Jam (TJ, white) marks somatic ICs, DAPI (blue) marks all nuclei, LaminC (red) marks Terminal Filament (TF) cells (cyan arrowheads in D-G) and Fas3 (also red) marks basal cells, except in **(A)** where red signal is just from Hts staining. All scale bars, 20 μm. **(A)** At 0h APF ovaries are not yet organized into distinct germaria. The germline (green) consists of individual cells intermingled with somatic IC precursor cells (white). The medial side of the ovary, on the right, has more developed Terminal Filaments. “Apical cells”, the precursors of epithelial sheath cells, are located at the apical (top) side of the ovary (white arrowhead). **(B)** At 12h APF ovaries are organized into distinct germaria, separated by a layer of migrating Apical cells. Lamin-C stains the nuclear envelope of Terminal Filament cells (cyan arrowhead). Fas3 staining is present on the medial side of the ovariole (pink arrowhead). TJ staining of somatic cells extends beyond the extent of the germline. **(C)** At 18h APF, basal stalks begin to form on the medial side of the ovary (pink arrowhead). **(D)** At 24h APF, Fas3 is spread more evenly around the circumference of the ovary, and stains a hub into which the posterior ends of the basal stalks converge. **(E)** By 30h APF, individual germaria are farther apart, separated from one another by a layer of 1-2 epithelial sheath cells. Lamin-C staining appears in the transition cell at the posterior end of the terminal filament, and dimly in epithelial sheath cells. **(F)** At 36h APF, germaria are separated by 2-3 epithelial sheath cells. Lamin-C expression is increased in epithelial sheath cells, and is also now visible in Cap cells (CC). Basal stalks (pink arrowheads in E-G) begin to narrow. **(G)** By 48h APF, the basal stalks have narrowed, and Fas3 begins to be expressed dimly in posterior ICs (yellow arrowhead). Lamin-C expression in the Cap cells increases at this stage. White arrowhead points to Lamin-C expression in epithelial sheath cells. **(H)** At 56h APF, germaria begin to bud the first egg chamber. **(I)** At 102h APF, 3-4 egg chambers have budded. **(J)** Cartoons illustrating individual germaria at 12h APF, 30h APF and adult stages for comparison. In the adult Escort Cells (ECs) surround developing germline cysts (white), three layers of Follicle Stem Cells (FSCs) ring the germarial circumference immediately anterior (left) to a stage 2b germline cyst and strong Fas3 (red) staining on the surface of early Follicle Cells (FCs).

Figure 2. Germline development during early pupal stages.

(A-F) Germline development at the indicated times after puparium formation (APF) was monitored with Hts (red), which stains spherical spectrosomes and branched fusomes in germline cells as well as the surface of many somatic cells, and Vasa (green), which identifies germline cells. The number of germline cells within a cyst was determined by examining the fusome connecting clustered Vasa-positive cells over a range of z-sections (here, single or small numbers of superimposed z-sections are shown). For each sample a close-up of the region outlined with white brackets is shown **(A'-F')** without or **(A"-F")** with the Vasa fluorescence channel. **(A-F)** Germaria progressively lengthen from anterior (apical, top, future anterior) to posterior (basal, bottom, future posterior) as germline cells become more numerous. The number of germline cells in a cyst is indicated as one (cyan arrowhead), two (white arrowhead), four (white arrow), eight (cyan arrow) or sixteen (yellow arrow). **(B-D)** Some germline cells migrate through the basal cells to become stranded at the posterior of the ovary. **(A-A'')** At 0h APF germline cells are single cells (cyan arrowheads) or 2-cell cysts (white arrowheads). **(B-B'')** At 12h APF the majority of germline cells have 1 or 2 cells, but posterior cysts may have 4 (white arrow) or 8 cells (cyan arrow). **(C-C'')** At 18h APF, there is a large range of germarial length and corresponding posterior cyst maturity. Longer germaria have 16 cells in posterior cysts (yellow arrows) whereas short germaria have only 2 cells in posterior cysts (white arrowhead). **(D-D'')** At 24h APF the majority of germaria have 16 cells in posterior cysts (yellow arrows) but the most posterior cyst has not yet moved beyond other cysts. **(E-E'')** At 36h APF a single cyst resides at the posterior of most germaria but in some cases the most posterior 16-cell cyst has not yet been resolved. **(F-F'')** By 48h APF each germarium has a single most posterior 16-cell cyst. Scale bars, 20 μm.

Figure 3. Common precursors for FSCs and ECs fate with derivatives clustered along the AP axis.

(A-K) GFP-labeled MARCM clones were induced from 6d to 2d before eclosion and flies were dissected 2d after eclosion. In each germarium labeled cells were scored as region 1 (r1) ECs, region 2a (r2a) ECs, or FSCs. **(A)** Most clones initiated 4-6d before eclosion contained only ECs (blue) or FSCs together with ECs (red), indicating a common precursor. Clones containing only ECs declined and clones containing FSCs but no ECs (green) increased in frequency when initiated at later times. **(B, C)** Data were pooled from clones induced from -4 to -6d. **(B)** Clones containing r1 ECs (n=174) were grouped according to the additional cell types they contained; inclusion of other r1 ECs was the most

frequent, and r2a ECs were more commonly included than more distant FSCs even though the total frequency of clones with r2a ECs (54%) and FSCs (57%) were similar. **(C)** Clones containing FSCs (n=155) contained r2a ECs more frequently than r1 ECs even though the total frequency of clones with r2a ECs (54%) was lower than for r1 ECs (64%). **(D-G)** Examples of different clones induced 5d before eclosion all demonstrate the clustering of marked cells (green) along the anterior (left) to posterior (right) axis. The anterior Fas3 (red) border, viewed in each z-section, allows distinction between FCs and FSCs (in the three layers anterior to Fas3); several z-sections were combined to show all labeled cells in one image. DAPI (white) staining reveals all nuclei but is omitted in **(D'-G')** and **(H-K)** for clarity. GFP-marked clones have **(D)** a cluster of r1 ECs (magenta arrows), **(E)** a cluster of r1 and r2a ECs (yellow arrows), **(F)** a cluster of r2a ECs and FSCs (blue arrows), **(G)** r1 and 2a ECs with FSCs. **(H-K)** Clones induced 2d before eclosion also showed clustering of progeny, with **(H)** r1 ECs only, **(I)** r1 and r2a ECS, **(J)** r2a ECs and FSCs, and **(K)** FSCs only. Scale bars, 20 μm.

Figure 4. Multicolor labeling of precursors shows clustering of progeny along the AP axis.

(A-F) Multicolor lineage tracing was performed by inducing clones 5d before eclosion and dissecting newly-eclosed flies. The anterior limit of Fas3 staining is marked by a white dashed line. Scale bar in **(A)** applies to all images, 20 μm. Precursors produce r1 (magenta) and r2a (yellow) ECs, FSCs (cyan), and FCs (red) in overlapping zones, indicated by the colored zones and in **(A-C)** arrow colors. **(A-C)** show examples of GFP-only clones, which are generated by two recombination events and are therefore infrequent. **(A)** A clone containing r1 and r2a ECs. **(B, B')** Different z planes of a germarium show a clone containing an r2a EC, FSCs, and FCs. **(C-C'')** Three z planes of a germarium showing a clone with r1 and r2a ECs and FSCs. **(D-F)** Examples of two clones of different colors in overlapping or adjacent zones, where arrow color indicates the clone color, not the cell type. **(D)** a GR (GFP plus RFP) clone (two-tone arrows) contains r1 ECs and Cap cells (extreme left) and a BR (*lacZ* plus RFP) clone (magenta arrows) contains r1 and r2a ECs. **(E)** A BR clone (magenta arrows) contains r1 ECs and a GR clone (yellow arrows) contains a r2a EC and an FSC. **(F)** A BR clone (magenta arrows) contains ECs and FSCs, and a BG (*lacZ* GFP) clone (cyan arrows) contains a r2a EC, FSCs and FCs.

Figure 5. Follicle Cell origins and deduced precursor numbers for ECs, FSCs and FCs.

(A-C) GFP-labeled MARCM clones (green) were induced 5d before eclosion and ovaries were dissected from newly-eclosed adults in order to detect all FCs produced during pupation. Fas3 is

stained in red and cell types are indicated with color-coded arrows, matching the labeled AP domains. Scale bar in **(A, B)**, 20 μm; **(A', C)**, 50 μm. **(A)** Germarium and **(A')** the rest of the ovariole of the same sample (the first egg chamber is in both images), showing a clone with marked ECs, FSCs and FCs (marked FCs are in the germarium and egg chambers 1-4. **(B)** A clone containing only ECs (no cells were marked in the rest of the ovariole). **(C)** A clone containing only FCs in egg chambers 2 and 3. **(D)** Distribution of clone types in GFP-only clones of multicolor flies and MARCM clones initiated 5d or 3.5d before eclosion, all examined in newly-eclosed adults. Clone types are: EC (EC-only), EC/FSC (ECs and FSCs, with or without FCs), FSC (with or without FCs), FC (FC-only), and EC + FC. Ovarioles with only marked ECs and FCs likely harbor two independent lineages. **(E)** Estimates of numbers of dividing precursor types at the time of clone induction for the same three lineage experiments as in **(D)**, after accounting for double-clones (see Methods and Table 2). Precursor types are defined by their adult products: pEC (only ECs), pEC/FSC (ECs and FSCs, with or without FCs), pFSC (FSCs with or without FCs), and pFC (only FCs).

Figure 6. FC founders per egg chamber and timing of FC recruitment to the first egg chamber.

(A-F) MARCM clones were initiated 5d or 3.5d before eclosion and examined in newly-eclosed adults**.** **(A, C)** Percentage of all ovarioles with FSC+FC lineages (blue) or FC-only lineages (orange) with marked FCs in the indicated locations (I: immediate FCs just posterior to FSCs, G: rest of the germarium: egg chambers 1-4) for clones induced **(A)** 5d or **(C)** 3.5d before eclosion. **(B, D)** Number of marked FC patches occupying the indicated percentages (in bins of 3%) of the whole FC epithelium of an egg chamber for all egg chambers labeled by FC-only lineages induced **(B)** 5d or **(D)** 3.5d before eclosion. **(E)** Distribution amongst egg chambers of FC-only clones induced 3.5d before eclosion. Each horizontal line denotes the location, designated as in **(A-C)**, of all marked FCs in a single ovariole. **(F, G)** FC-only clones (green) induced at -3.5d were commonly present **(F)** only in egg chamber 4 or **(G)** in egg chambers 3 and 4. Fas3: red. Scale bars, 50 μm.

Figure 7. Discovery of Extra-Germarial Crown Cells (EGCs); a potential source of early FCs.

(A-G) Traffic Jam (TJ) positive cells (white) were counted in ovaries stained also for Vasa (green), LaminC and Fas3 (both in red), and DAPI (blue). Bar, 20 μm applies to all images. **(A-D)** From 0h-48h APF, prior to budding of the first egg chamber, ICs, defined as intermingled with germline cells (green) in the developing germarium, expressed TJ but little or no detectable Fas3. Cells posterior to the

developing germaria expressed Fas3 and were previously all termed basal cells and expected to intercalate to form the basal stalk. However, a subset of Fas3-positive cells immediately posterior to the germarium also expressed TJ. Those cells formed an Extra-Germarial Crown of increasing cell numbers, indicated by green brackets. Average IC and EGC cell numbers were derived from counting **(A)** 5, (**B)** 5, (**C)** 10 and (**D)** 5 samples. **(D)** At 48h APF the most posterior cyst (green) appears to have invaded EGC territory, with surrounding cells indicated with yellow brackets. (**E-G)** Three developing ovarioles from the same 56h APF ovary, representing progressively later stages of development from top to bottom, show the most posterior cyst leaving the germarium and surrounded by Fas3-positive, TJ-positive cells. **(E, F)** Fas3-positive, TJ-positive cells posterior to the cyst (green bracket), and around the cyst (yellow bracket) were counted for these single samples and then **(G)** as on the cyst (magenta bracket) or anterior to the cyst and forming a secondary EGC posterior to the germarium (blue bracket) Those two populations are separated by stalk cells that do not stain for TJ. (**H)** Tabulation of the number of cells scored in the regions indicated by colored brackets (BC: budded egg chamber).

Figure 8. ICs move independently of one another and do not mix with EGCs.

(**A**) Z-projection of selected time-points from live imaging of a 30h-APF ovary for 6h 30min, showing five tracked ICs. ICs were located at the outer surface of the germarium and moved independently of one another in posterior, anterior, and lateral directions (around the circumference). The most posterior germline cyst (outlined by a white dotted line) moved posteriorly past the cyan and yellow IC cells. The relative disposition of ICs and cysts changed considerably, suggesting they are not strongly associated. Only z planes containing tracked cells were included in the projection (z4, 5, 6, 7, and 8 at 00:00 and z5, 6, 9, and 10 at 06:30) **(A')** Individual z sections of the 30h-APF ovary (arranged horizontally for each time point) show that ICs move around the circumference of the germarium. The cyan and yellow cells began on the bottom of the germarium and moved towards the mid-section, whereas the pink and white cells started in a mid-section and moved to the bottom. (**B)** Z-projection of selected time-points from live imaging of a 40h-APF ovary for 7h 15min, showing five tracked ICs. ICs moved independently of one another and remained in their domain as the most posterior germline cyst (highlighted in white) moved past. Four cells in the EGC (outlined red cells) remained in the EGC (indicated by the yellow bracket). Projected sections are z5-9 at 00:00 and z4, 7, 8 and 9 at 07:15. (**B')** Individual z sections of the 40h-APF ovary show that IC cells move independently in all directions, and EGC cells did not move relative to one another, suggesting greater cohesion.

Figure 9. Budding of the first egg chamber: EGC cells become FCs.

Time-stamped frames from a 3D reconstruction of a movie of 14h 45 min starting at 48h APF and showing budding of an egg chamber. All cells are labeled green from a *ubi-GFP* transgene. Three cells that were visible near the surface of a 3D reconstruction are colored in red, pink, and yellow in the lower germarium, together with three other cells (open circles) that were in interior z slices. All marked cells were tracked using Zeiss Zen software for 60 time points over 14h 45 min, except for the red cell which could not be reliably tracked after 10h and the yellow cell in the lower germarium, which was not tracked before 5h 45min. The posterior germline cyst in the lower germarium is highlighted in green. Cyst cells were distinguishable from somatic because the nuclei were larger and paler green. The cyst slid past adjacent ICs, which ended up either on the cyst (red, pink cells from lower germarium) or (yellow cell in top germarium) anterior to the cyst in a secondary EGC (pink bracket). The cyan cell in the primary EGC (indicated by yellow brackets) adopted progressively more anterior positions on the germline cyst after the cyst moved into EGC territory. The white cell was originally in a location posterior to the EGC (and is expected, from fixed images, not to express TJ) but then moved into EGC territory by 3h 45min and ended up close to the cyan cell on the budded germline cyst. The location of the cyan and white cells covering the posterior of the cyst can be seen clearly in Fig. S3. The yellow cell in the upper germarium was initially located immediately anterior to the posterior cyst and moved into the secondary EGC (magenta brackets), as seen more clearly in Fig. S2A, B. Individual z-slices showing the locations of the red, pink and yellow cells at the beginning, middle, and end of their imaging times are shown in Fig.S2C. Time is in hours:minutes.

Figure 10. FLY-FUCCI labeling shows progressive accumulation of anterior ICs in G1 or a G0 arrest.

(A-G) *C587-GAL4* was used to drive *UAS-FUCCI* expression and ovaries were stained for Fas3 (white) and TJ (not shown) to identify all somatic cells. Somatic cells were either green (G1 or G0), red (late S phase), red/green (G2) or without any color (early S-phase for cells with adequate *C587-GAL4* expression). Germaria are outlined with dotted lines. All bars, 20 μm. **(A-F)** Many red or red/green cells are present in anterior locations close to Cap Cells at **(A)** 12h APF and **(B)** 18h APF (arrows) but **(C)** by 24h APF and **(D)** 36h APF fewer such cells are evident and they are further from the anterior (arrows). **(E)** At 48h APF ICs in the anterior third of the germarium are uniformly green (G1 or G0). The

bracketed region is magnified with enhanced colors to reveal **(E')** that many cells in the EGC are red (S-phase), while one or two more posterior, basal stalk cells are faintly green but *C587-GAL4* expression is low at these locations. **(F)** At 96h APF, after three egg chambers have budded (two are outlined with blue dotted lines), red/green ICs can still occasionally be seen in the anterior half of the germarium (arrows) but **(G)** in adults this territory, occupied by r1 ECs, is entirely green, followed by a mix of green and red/green more posterior r2a ECs, and FSCs, which are predominantly red/green (G2), red or colorless (S-phase) and with only a few green (G1) cells. In adults, *C587-GAL4* expression ends at the FSC/FC border.

Figure 11. Lineages induced by bond-GAL4 reveal typical IC precursor patterns and a later EGC contribution.

(A-G) bond-GAL4/G-TRACE clones (green) were examined in 0-12h adult ovaries, stained with antibodies to Fas3 (white in **(A-C)**) and DAPI (white in **(F, G)**). **(A-C)** For animals maintained at 18C throughout development, we observed mainly **(A)** marked ECs only or **(B, C)** marked ECs, FSCs and FCs; scale bars, 20 μm. **(D)** Distribution of clone types observed for animals kept at 18C throughout (green), raised at 29C and moved to 18C 2d after pupariation ("29C larval", blue), raised at 18C and moved to 29C for the last 3-4d of pupation ("29C pupal", yellow), or the aggregate of all results (pink). EC/FSC and FSC categories almost always included FCs also. **(E)** Estimates of precursor numbers for MARCM clones induced 5d before eclosion (blue) and for the aggregate of all bond-Gal4 lineages (pink) after disaggregating raw data into single lineages (see Methods). **(F)** Posterior egg chamber (29C larval) with small GFP clones (arrowheads). Multiple z-sections are projected to show all clones. **(G)** Posterior egg chamber (29C pupal) with patches of **(G')** GFP-positive cells, some of which also express **(G")** RFP, indicating relatively recent expression of bond-GAL4. RFP+ clone. **(F-G)** Scale bars, 50 μm.

Figure 12. Development of a Wnt signaling gradient in pupal germaria.

(A-L) Ovaries from pupae expressing Fz3-RFP as a reporter for Wnt pathway activity were stained for Fas3 (white) and imaged intact. **(A)** Individual germaria (highlighted) are shown in **(D-F)** and **(J-L)**, oriented anterior (left) to posterior (right), with the germarial region (containing germline cells) outlined in yellow and the anterior border of strong Fas3 staining indicated by a blue arrowhead. **(B, C, G-I)** RFP

intensities (y-axes) were measured over 5 μm intervals along the edge of the germarium where most somatic cells are located, starting adjacent to Cap Cells (x-axes). Fz-RFP profiles, showing mean and SEM were derived from germaria at **(B)** 27h APF (n=50 cells in 7 germaria), **(C)** 36h APF (n=108 cells in 14 germaria), **(G)** 48h APF (n=138 cells in 15 germaria), **(H)** 60h APF (n=178 cells in 14 germaria) and **(I)** adults (n=178 cells in 14 germaria). The average location of the border of strong Fas3 expression (blue vertical line), Fz3-RFP levels at that location (horizontal line) and the location of the average posterior end of the germline (green vertical line; measured from the Cap cells to the central point at the posterior of the germline) are indicated. **(D-F, J-L)** Multiple z-sections were projected to show Fz3-RFP in cells along the length of germaria. **(D)** Fz3-RFP was not detected at 21h APF, **(E)** was present at low levels with an anterior bias at 27h (4 μm-thick z projection) and **(F)** at 36h APF (5 μm-thick z projection) before **(J)** accumulating to high anterior levels with a steep decline ending close to the strong Fas3 border at 48h APF (4 μm-thick z projection) and **(K)** 60h-APF (5 μm-thick z projection), similar to **(L)** the profile in newly-eclosed adults (10 μm-thick z projection). Scale bar of 20 μm applies to all images

Figure 13. Wnt and Jak/STAT signaling influence precursor cell position.

(A-M) MARCM lineages with genetically altered Wnt and JAK/STAT pathway activity were induced (A-F) from -6d to -2d before eclosion and examined in 2d-old adults or **(G-M)** 5d before eclosion and examined in newly-eclosed adults. **(A-C)** The total number of marked cells of each cell type (r1, r2a, or FSCs) was counted over all samples and expressed as a percentage of all marked ECs and FSCs for control clones (red), *arr* mutant clones lacking Wnt pathway activity (blue) and *axn* or *apc* mutant clones (combined data, gold) with increased Wnt pathway activity. **(D-F)** Images of germaria stained for Fas3 (red) show examples of a **(D)** control lineage with all cell types labeled, **(E)** an *arr* lineage with only marked r2a ECs and FSCs and **(F)** an *axn* lineage with only marked r1 and r2a ECs. Bar, 20 μm. **(G-M)** For clones induced 5d before eclosion and analyzed in 0d-old flies, **(G)** the total number of marked cells of each cell type (r1, r2a, or FSCs) was counted over all samples and expressed as a percentage of all marked ECs and FSCs for control clones (gold), clones expressing dnTCF to reduce Wnt pathway activity (blue), *axn* mutant clones with increased Wnt pathway activity (red) or *stat* mutant clones lacking JAK-STAT pathway activity (green). **(H)** Distribution of clone types for the MARCM lineages described in (G): EC (EC-only), EC/FSC (with or without FCs), FSC (with or without FCs), FC (FC-only). **(I-M)** Images show lineage examples for **(I)** control **(J)** *UAS-dnTCF*, **(K)** *stat* and **(L, M)** *UAS-Hop* (to increase JAK-STAT pathway activity). **(L, L')** Increased JAK/STAT signaling caused ectopic

Fas3 expression (red, anterior to the normal Fas3 border marked by arrowheads) in marked cells. The Fasciclin3 border has shifted far anterior and is marked with red arrowheads (L' is Fas3 alone). **(M)** Two ovarioles with many marked cells (green) expressing *UAS-Hop*. Germaria are indicated by white brackets, the normal anterior border of Fas3 by red arrowheads and DAPI-stained nuclei are in blue.

Figure 14. Summary of precursor lineage development.

Cartoon of the fate of single precursor types from 0h APF until 60h APF deduced from lineage studies and pupal ovary imaging. Most precursors (green) generate only adult ECs, with more anterior (left) precursors producing only r1 ECs (top row) and more posterior precursors also producing r2a ECs and more cells in total (second row). Filled green cells have ceased division. Most FSC-producing precursors also produce ECs. A few, more anterior precursors (third row) produce no FCs but most (fourth row) also produce FCs. Precursors that produce adult FSCs but no ECs also produce FCs (fifth row). Precursors at the posterior of developing germaria produce only FCs. A subset of their progeny accumulate posterior to the germarium from 24h APF onward in the EGC and most cells in the EGC will become FCs of the first budded egg chamber. More posterior precursors produce larger numbers of progeny because anterior cells divide more slowly and arrest division prior to eclosion.

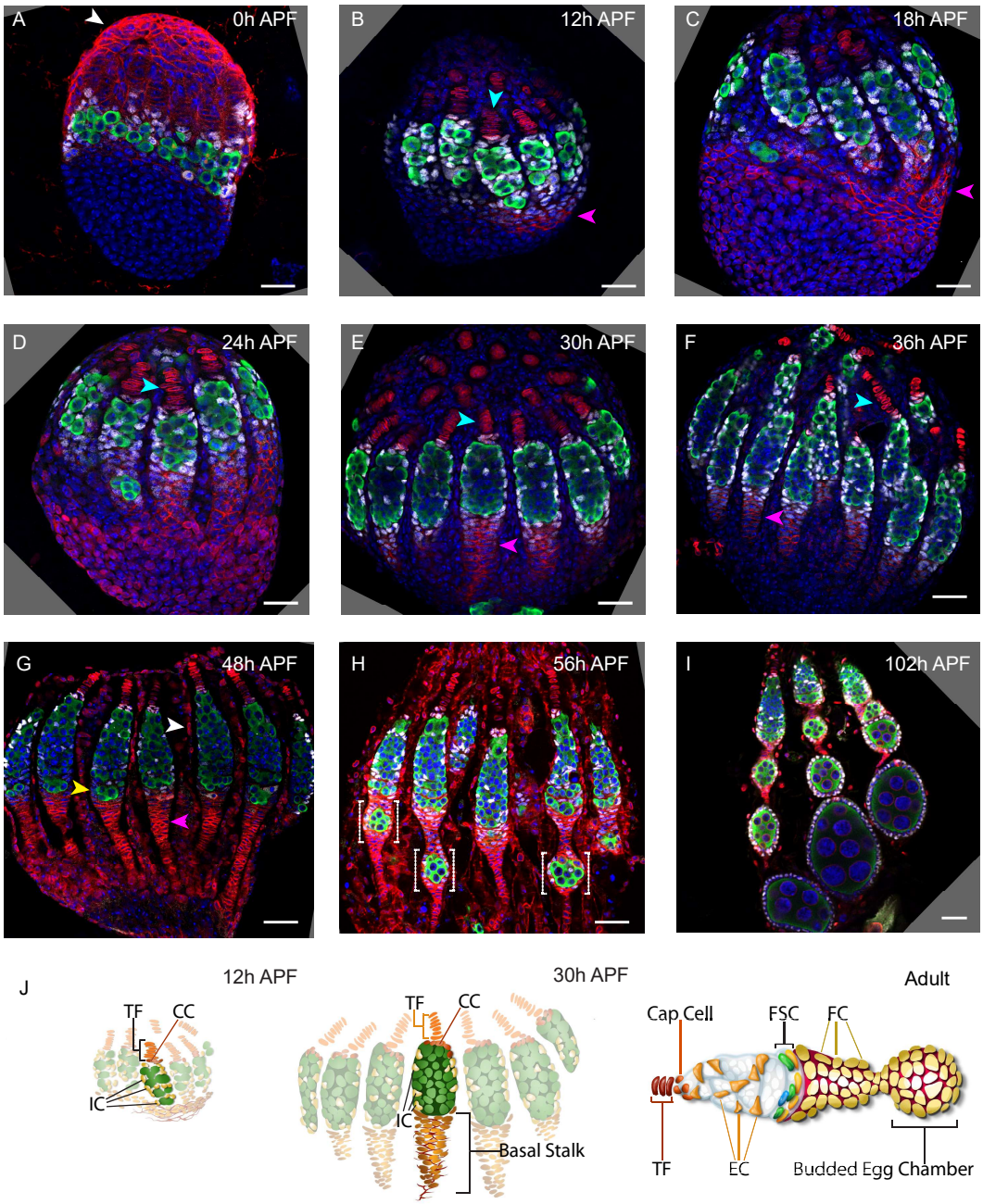

Figure 1

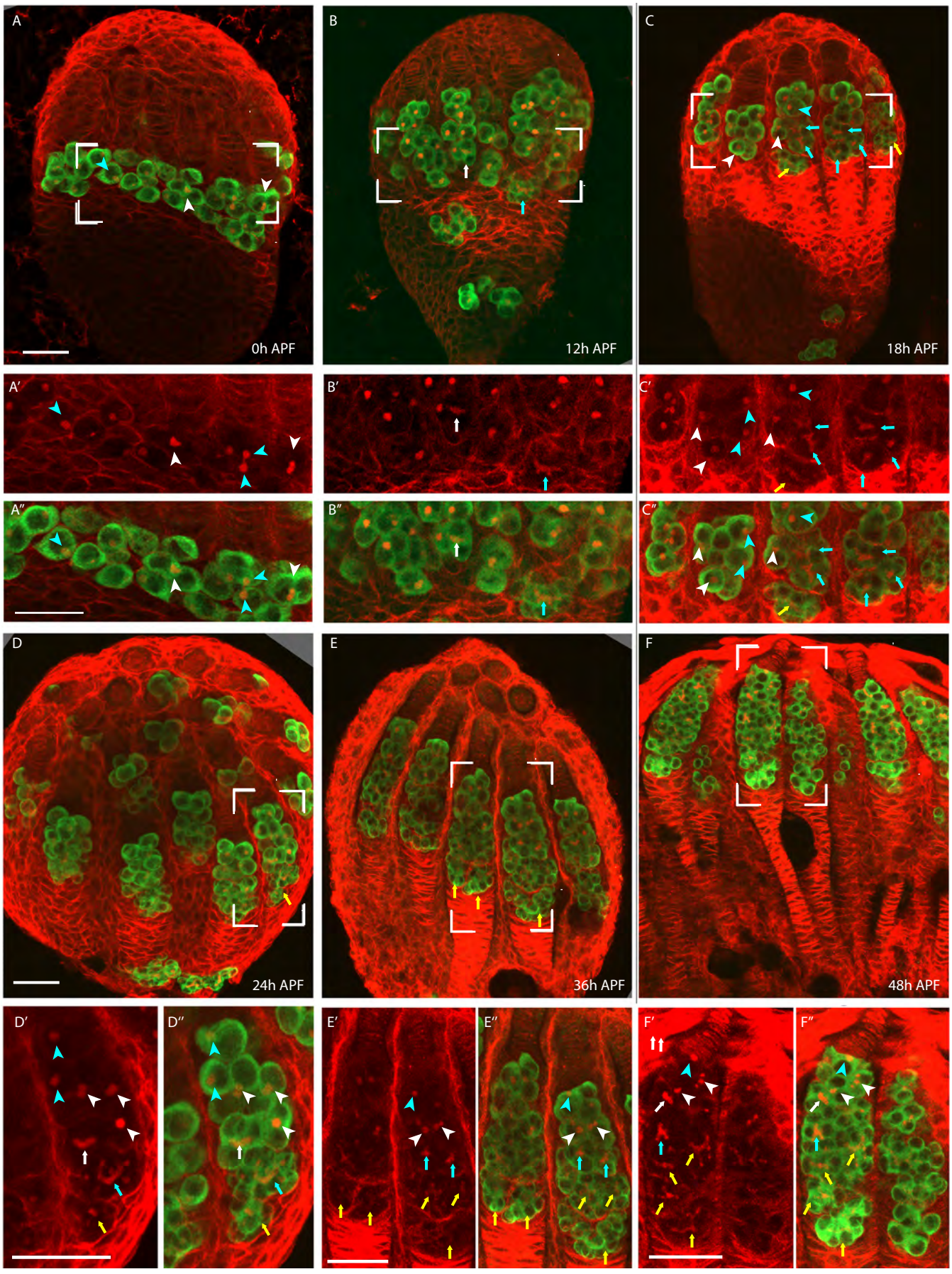

Figure 2

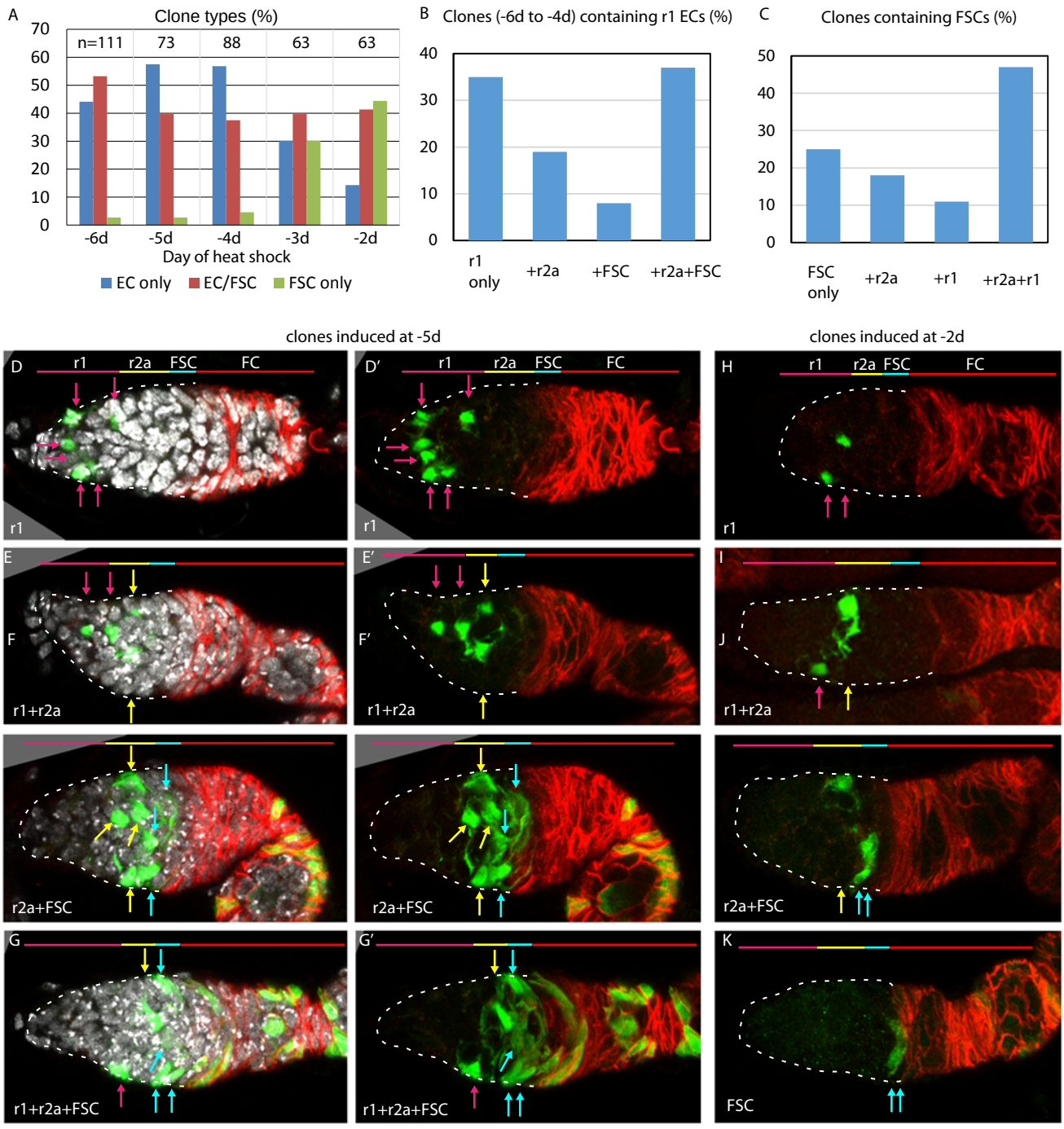

Figure 3

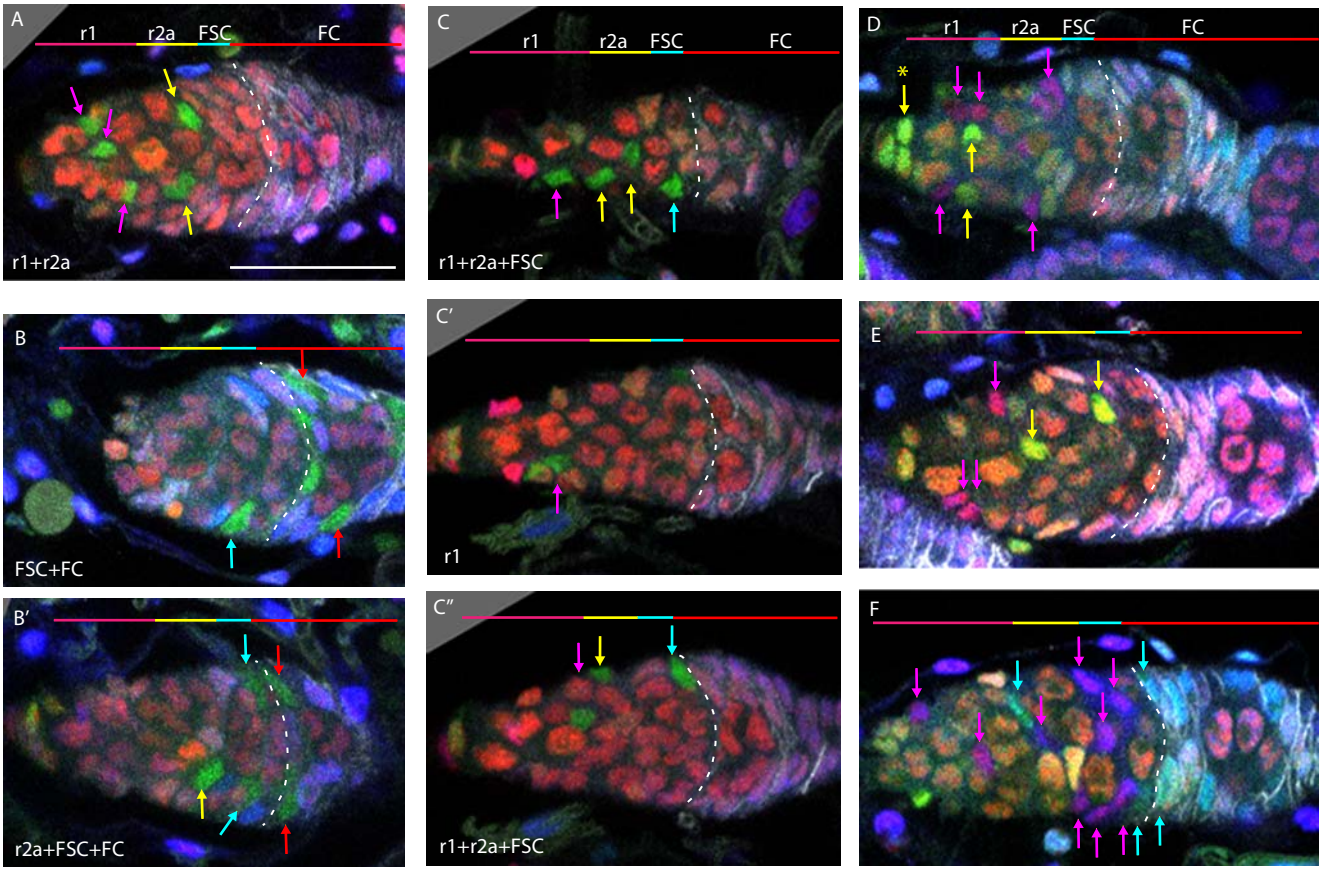

Figure 4

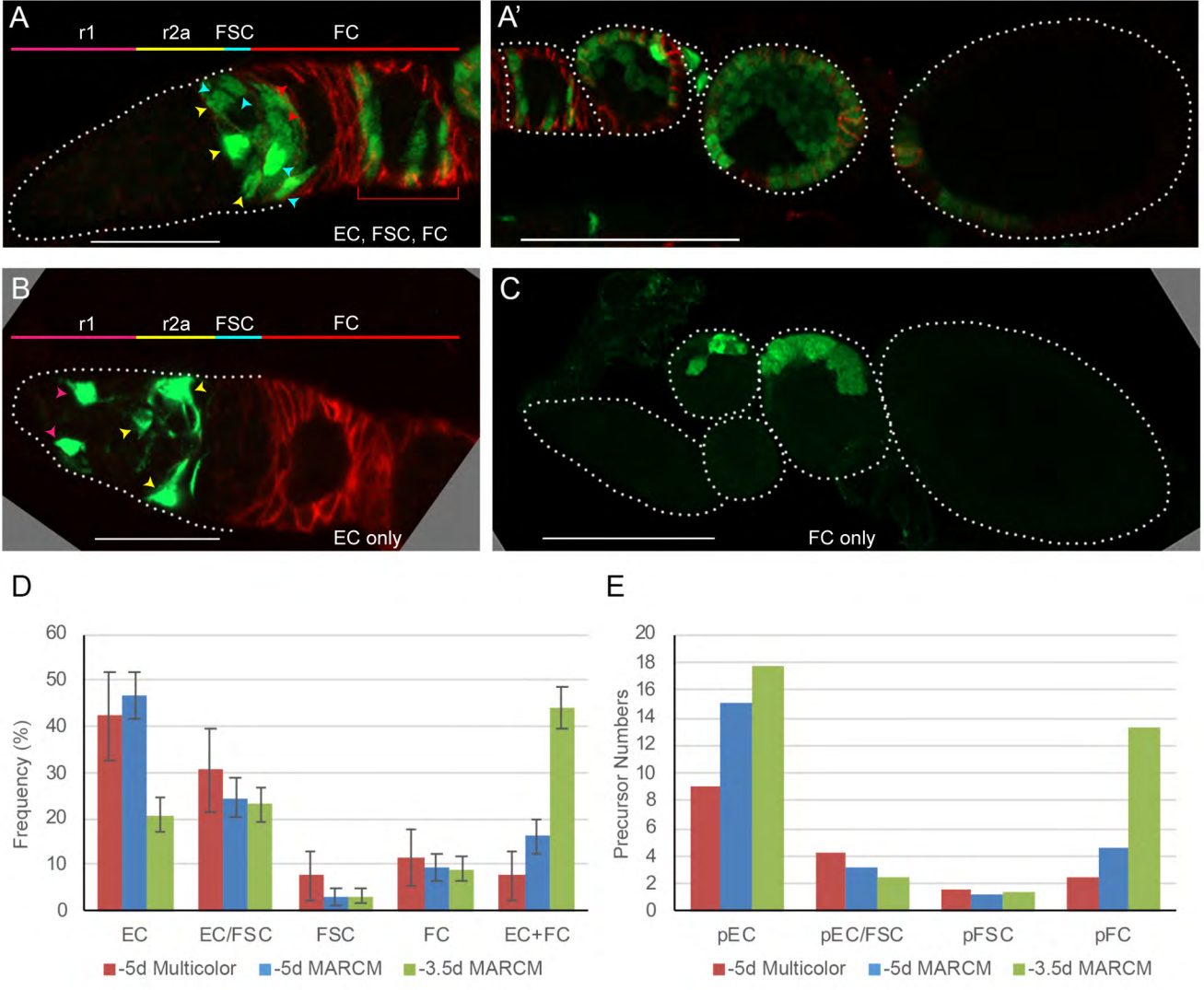
A
r1
r2a
FSC
FC
EC, FSC, FC
A'
B
r1
r2a
FSC
FC
EC only
C
FC only
D
Frequency (%)
60
50
40
30
20
10
0
EC
EC/FSC
FSC
FC
EC+FC
-5d Multicolor
-5d MARCM
-3.5d MARCM
E
Precursor Numbers
20
18
16
14
12
10
8
6
4
2
0
pEC
pEC/FSC
pFSC
pFC
-5d Multicolor
-5d MARCM
-3.5d MARCM

Figure 5

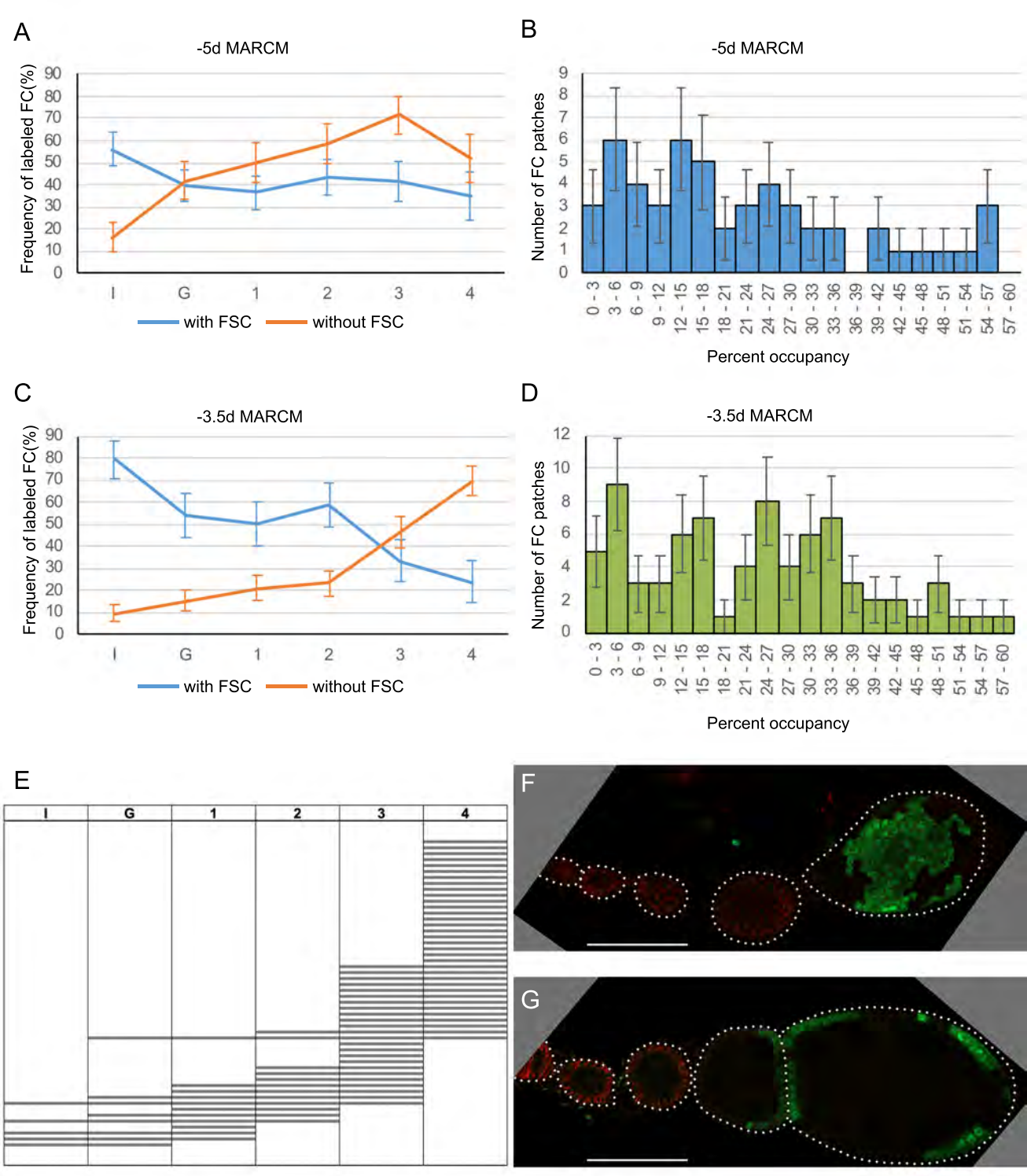
A
-5d MARCM
Frequency of labeled FC(%)
90
80
70
60
50
40
30
20
10
0
I
G
1
2
3
4
with FSC
without FSC
B
-5d MARCM
Number of FC patches
9
8
7
6
5
4
3
2
1
0
0 - 3
3 - 6
6 - 9
9 - 12
12 - 15
15 - 18
18 - 21
21 - 24
24 - 27
27 - 30
30 - 33
33 - 36
36 - 39
39 - 42
42 - 45
45 - 48
48 - 51
51 - 54
54 - 57
57 - 60
Percent occupancy
C
-3.5d MARCM
Frequency of labeled FC(%)
90
80
70
60
50
40
30
20
10
0
I
G
1
2
3
4
with FSC
without FSC
D
-3.5d MARCM
Number of FC patches
12
10
8
6
4
2
0
0 - 3
3 - 6
6 - 9
9 - 12
12 - 15
15 - 18
18 - 21
21 - 24
24 - 27
27 - 30
30 - 33
33 - 36
36 - 39
39 - 42
42 - 45
45 - 48
48 - 51
51 - 54
54 - 57
57 - 60
Percent occupancy
E
I
G
1
2
3
4
F
G

Figure 6

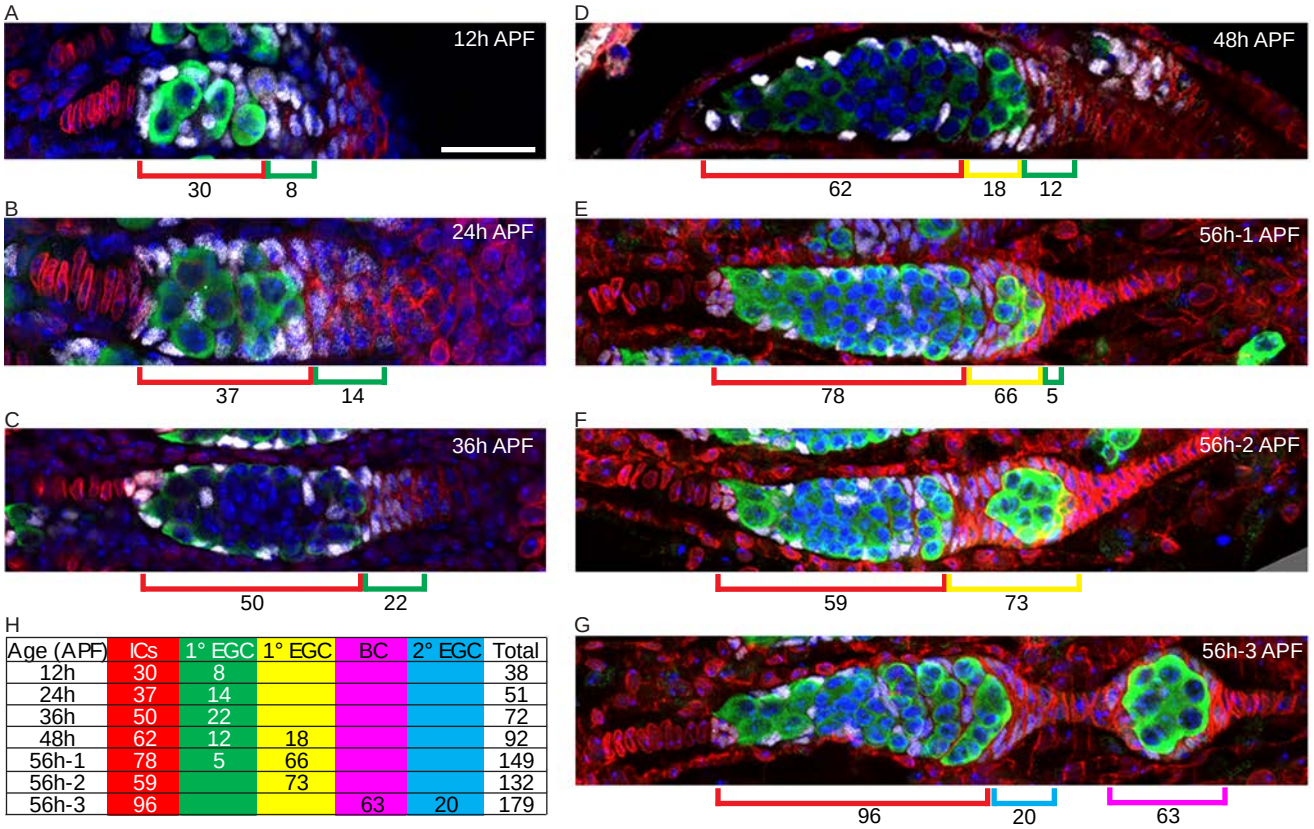

H

Age (APF)	ICs	1° EGC	1° EGC	BC	2° EGC	Total
12h	30	8				38
24h	37	14				51
36h	50	22				72
48h	62	12	18			92
56h-1	78	5	66			149
56h-2	59		73			132
56h-3	96			63	20	179

Figure 7

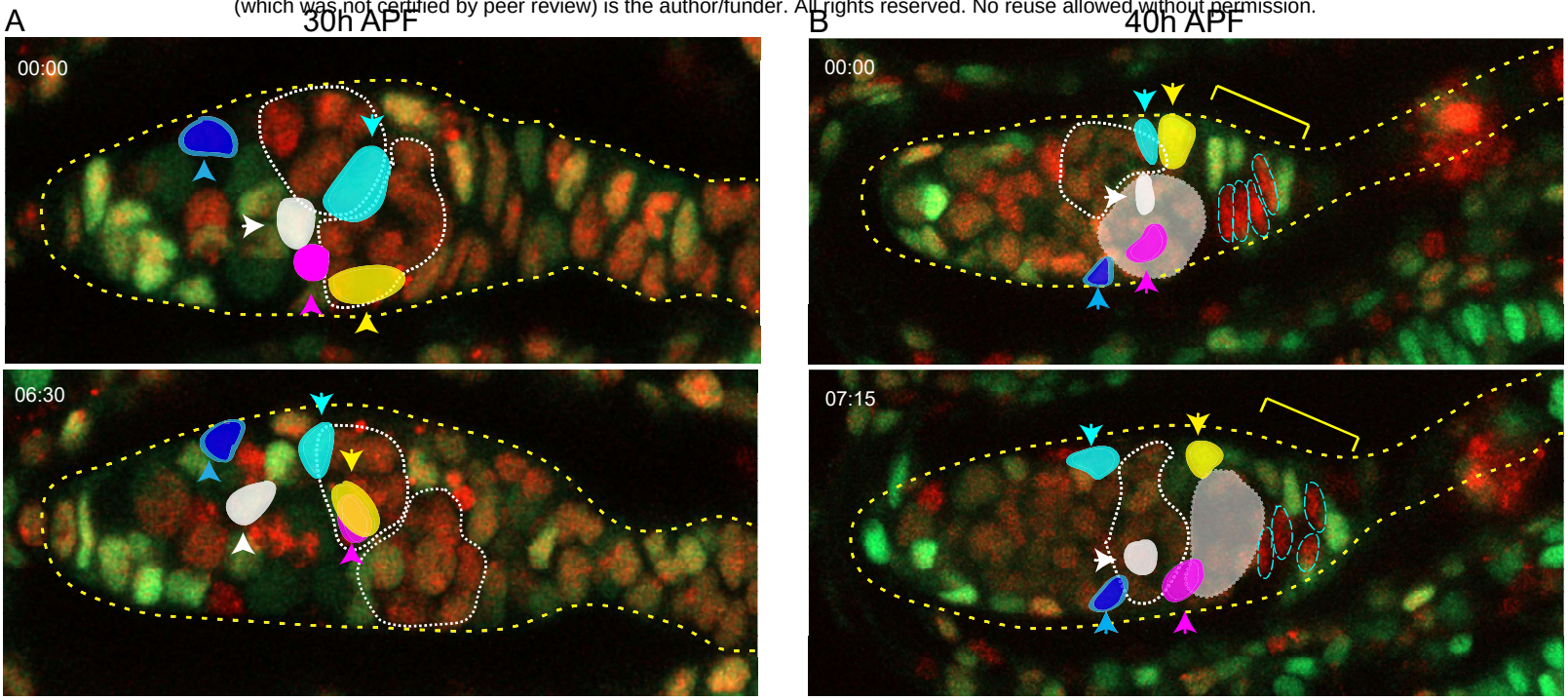

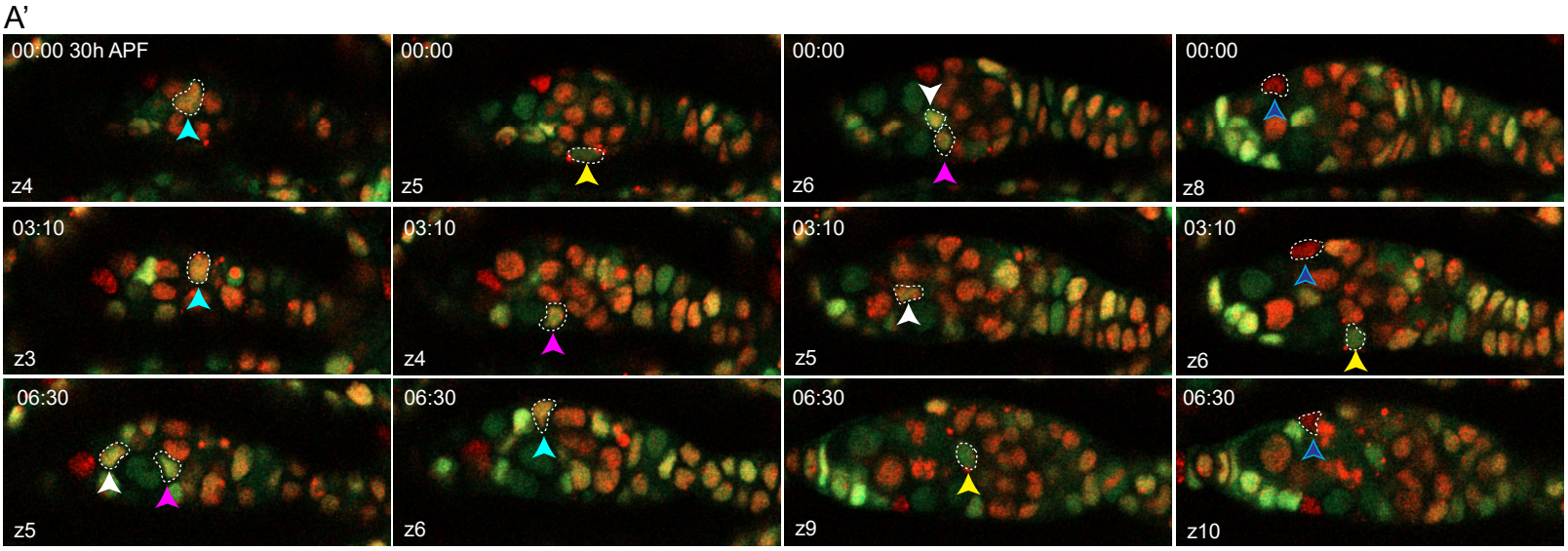

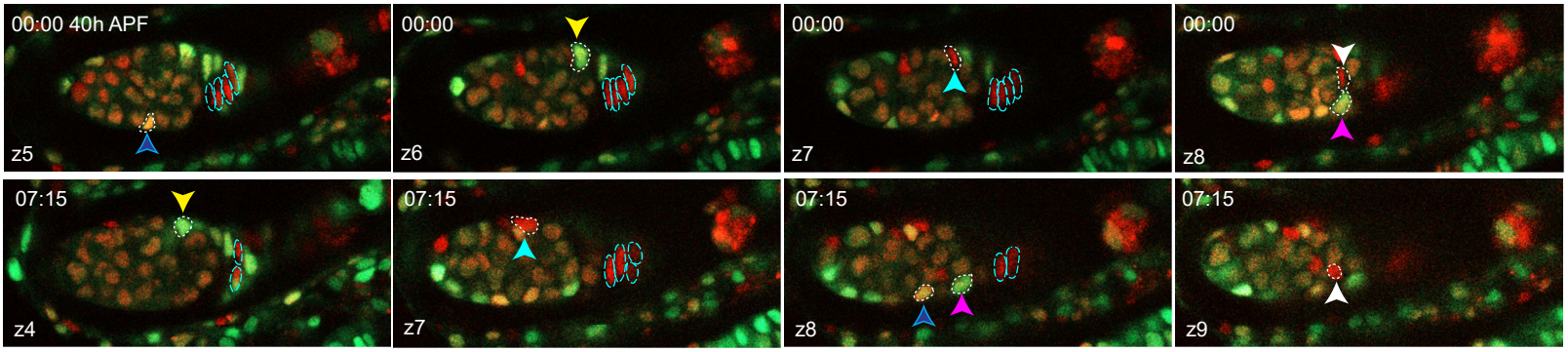

Figure 8

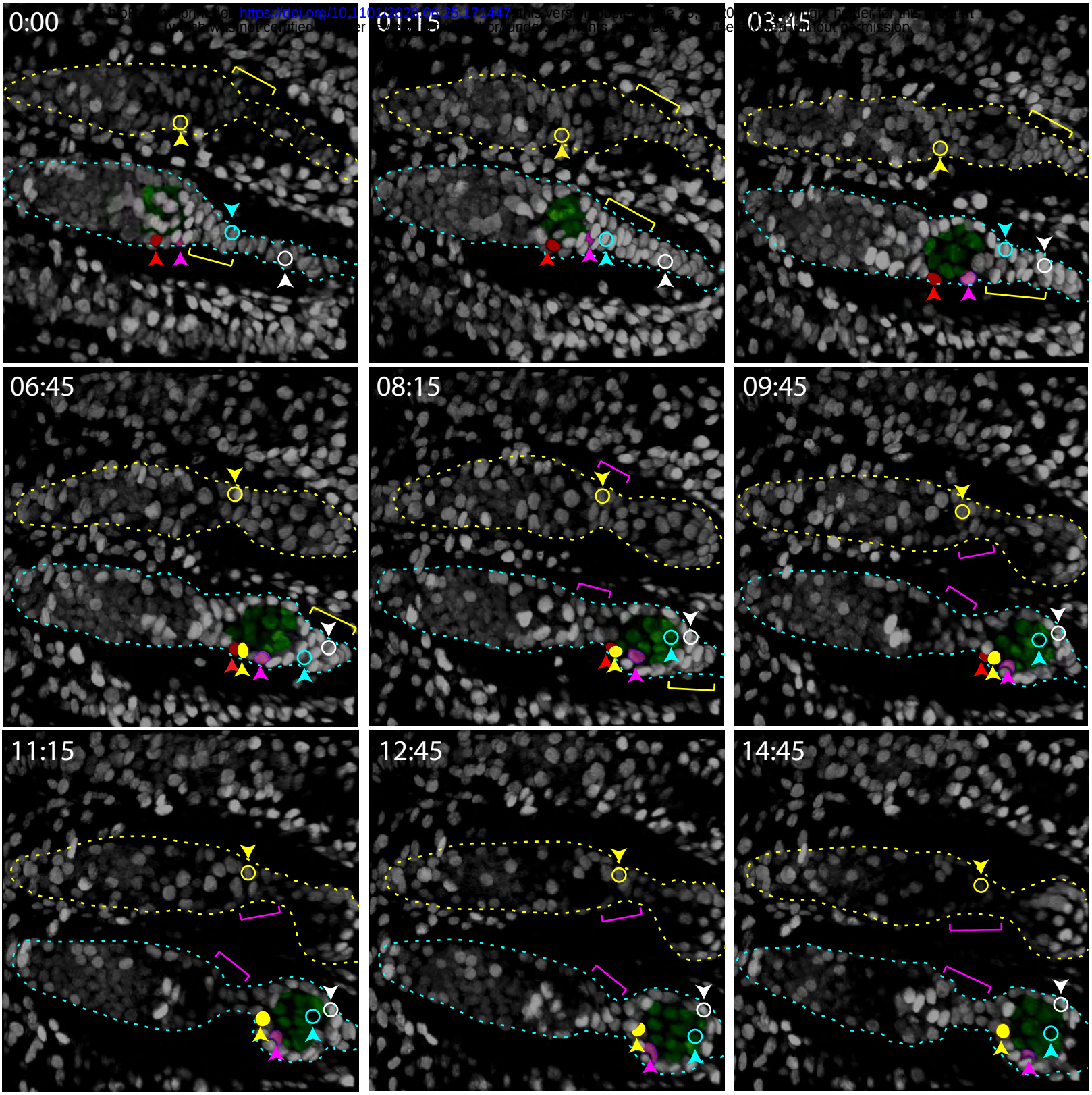

Figure 9

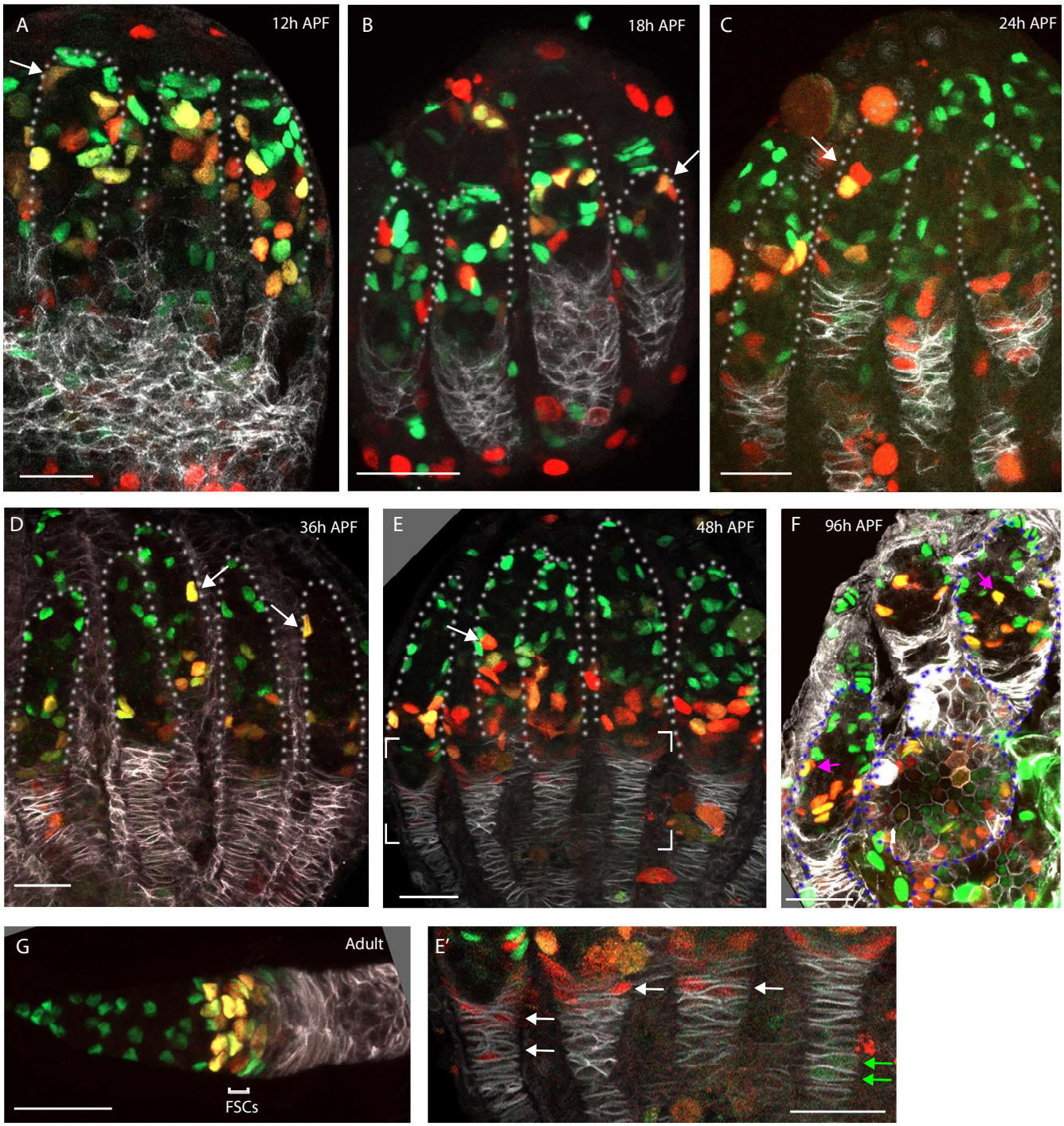

Figure 10

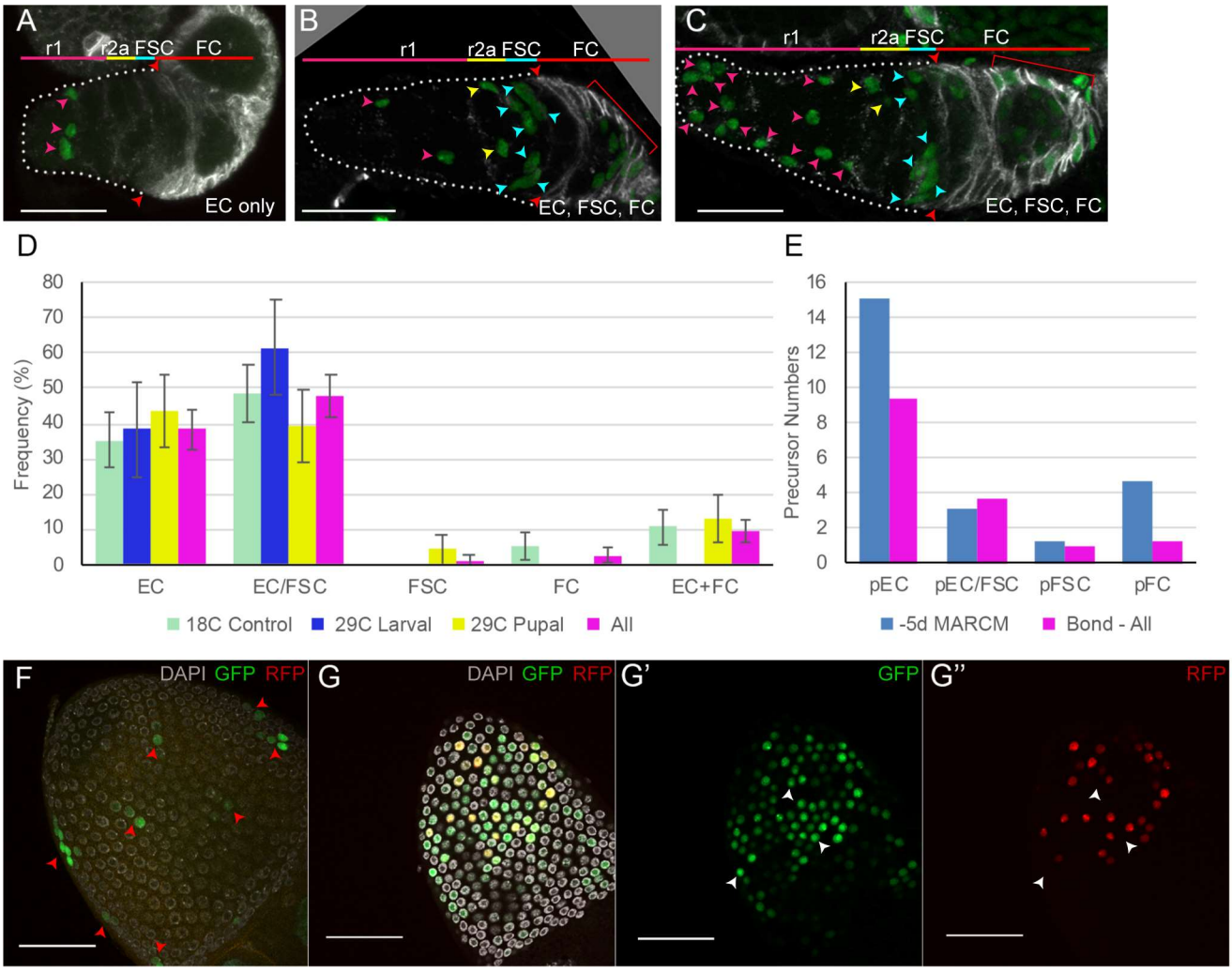

Figure 11

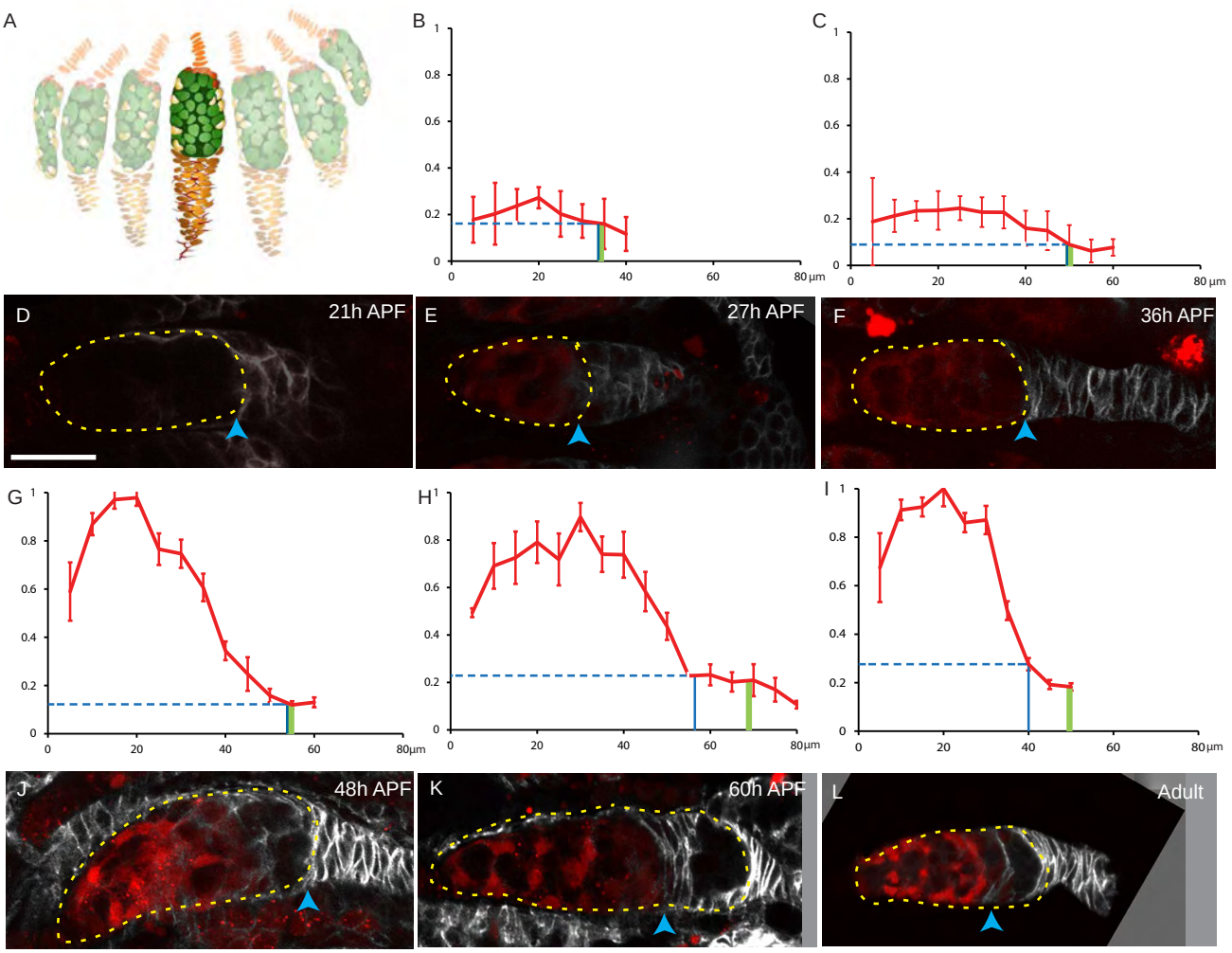
A
B
C
D
21h APF
E
27h APF
F
36h APF
G
H
I
J
48h APF
K
60h APF
L
Adult
80 µm

Figure 12

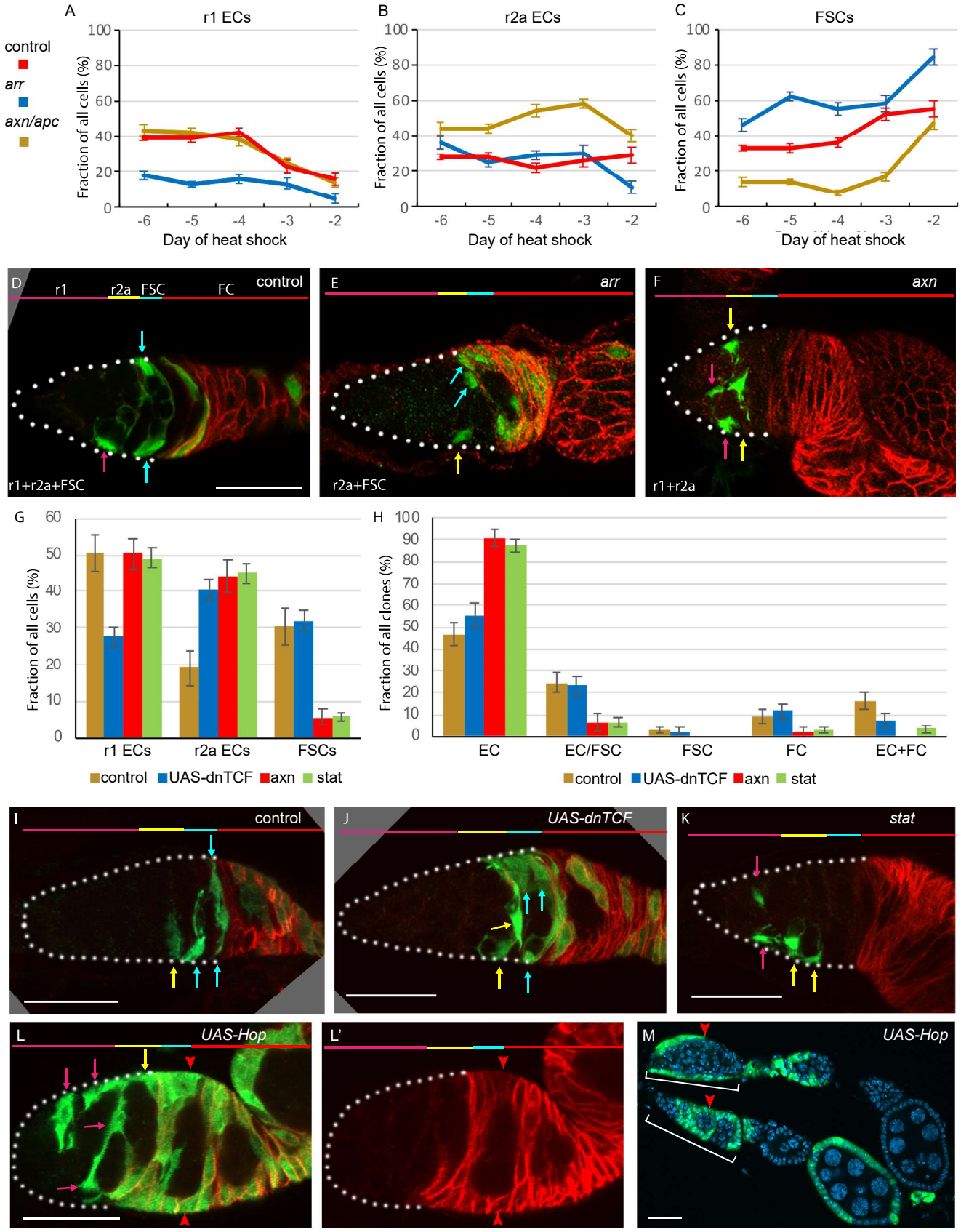

Figure 13

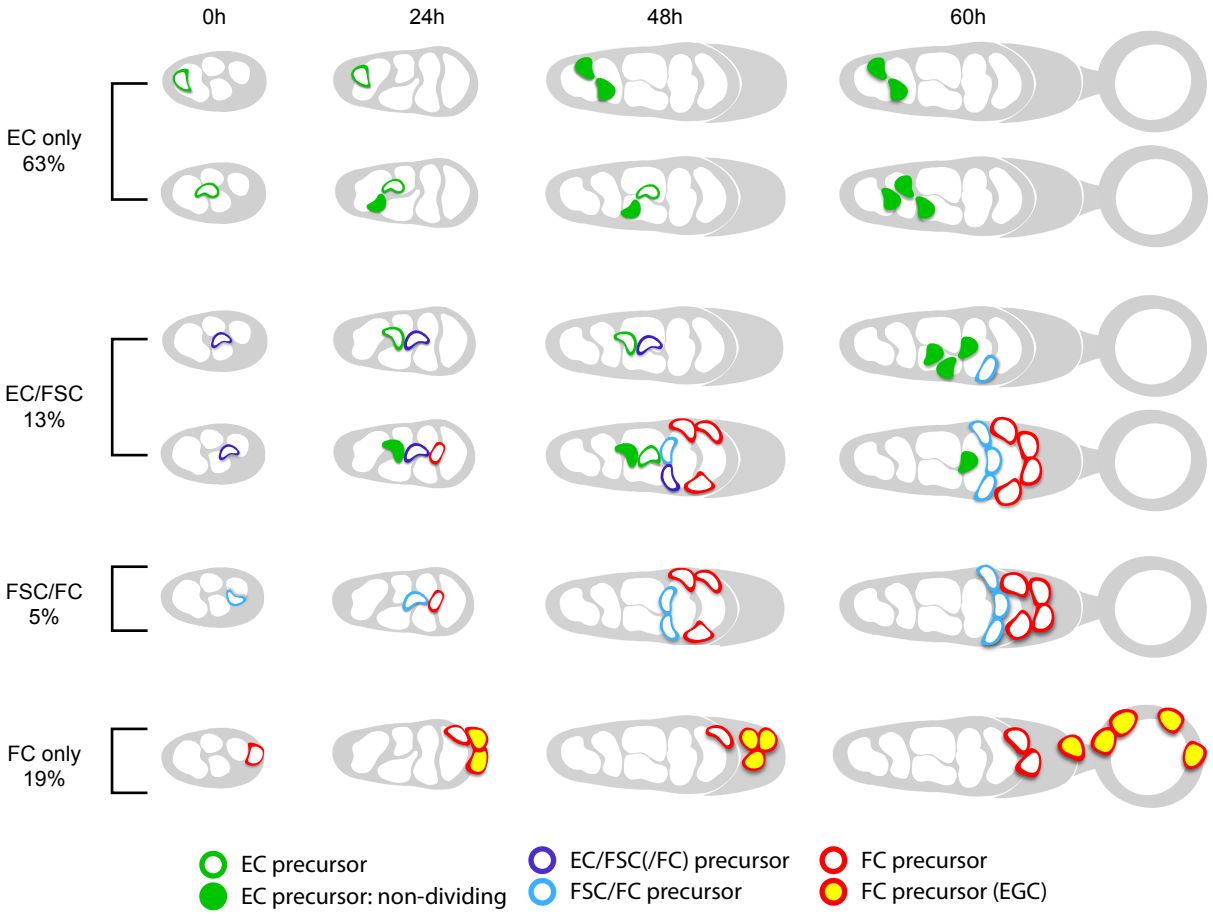
0h
24h
48h
60h
EC only
63%
EC/FSC
13%
FSC/FC
5%
FC only
19%
EC precursor
EC precursor: non-dividing
EC/FSC(/FC) precursor
FSC/FC precursor
FC precursor
FC precursor (EGC)

Figure 14